

LimTDD: A Compact Decision Diagram Integrating Tensor and Local Invertible Map Representations

Xin Hong¹, Aochu Dai², Dingchao Gao¹, Sanjiang Li³, Zhengfeng Ji², Mingsheng Ying³

¹Key Laboratory of System Software (Chinese Academy of Sciences) and State Key Laboratory of Computer Science, Institute of Software, Chinese Academy of Sciences, China

²Department of Computer Science and Technology, Tsinghua University, China

³Centre for Quantum Software and Information, University of Technology Sydney, Australia

Abstract—Tensor Decision Diagrams (TDDs) provide an efficient structure for representing tensors by combining techniques from both tensor networks and decision diagrams, demonstrating competitive performance in quantum circuit simulation and verification. However, existing decision diagrams, including TDDs, fail to exploit isomorphisms within tensors, limiting their compression efficiency. This paper introduces Local Invertible Map Tensor Decision Diagrams (LimTDDs), an extension of TDD that integrates local invertible maps (LIMs) to achieve more compact representations. Unlike LIMDD, which applies Pauli operators to quantum states, LimTDD generalizes this approach using the XP-stabilizer group, enabling broader applicability. We develop efficient algorithms for normalization and key tensor operations, including slicing, addition, and contraction, essential for quantum circuit simulation and verification. Theoretical analysis shows that LimTDD surpasses TDD in compactness while maintaining its generality and offers exponential advantages over both TDD and LIMDD in the best-case scenarios. Experimental results validate these improvements, demonstrating LimTDD’s superior efficiency in quantum circuit simulation and functionality computation.

Index Terms—Tensor Decision Diagrams, Local Invertible Maps, Quantum Circuits, Tensor Networks

I. INTRODUCTION

QUANTUM computing has experienced rapid development in recent years, offering potential breakthroughs in cryptography [13], optimization [15], quantum chemistry [5], and more. As quantum hardware scales, the need for efficient simulation and verification of quantum circuits becomes increasingly critical. Decision diagrams have emerged as a powerful approach for these tasks, enabling compact representations and efficient manipulations of quantum states and operations.

Various decision diagram structures have been introduced, including Quantum Information Decision Diagrams (QuIDD) [16], Quantum Multiple-Valued Decision Diagrams (QMDD) [12], X-Decomposition Quantum Decision Diagrams (XQDD) [20], and Tensor Decision Diagrams (TDD) [8]. These decision diagrams have been successfully applied in the simulation and verification of quantum circuits [17], [3], [4], as well as quantum state preparation [10] and quantum circuit design automation [22]. Among these, QuIDD introduces the method of classical algebraic decision diagrams [1] to handle

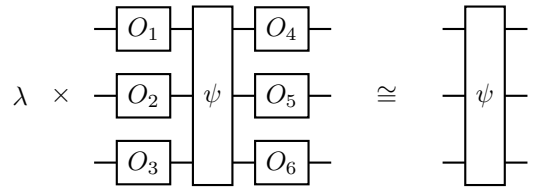


Fig. 1. Tensor isomorphism, where $\lambda \neq 0$ is a complex number and each O_i is an invertible operator.

quantum information, QMDD takes advantage of the unique form of quantum circuits, XQDD fully exploits the commonly used symmetries in quantum gates, while TDD leverages both tensor network techniques and decision diagram methodologies, enabling efficient compression and representation of tensor structures in quantum circuits. What is worth mentioning is that, by optimizing the contraction order of the tensor network, TDD has the potential to further enhance computational efficiency [23]. Recently, TDD has also been employed in the approximate equivalence checking of noisy quantum circuits [7] and equivalence checking of dynamic quantum circuits [6].

While TDDs provide a structured and compact representation, they do not explicitly exploit isomorphic structures within tensors. Two tensors are considered *isomorphic* if they encode the same essential information up to a (nonzero) global coefficient and a local transformation applied to each index (see Fig. 1 for an illustration). Recognizing and exploiting such isomorphic relationships may enable significant compression, as structurally similar tensors can be merged into a single representation. However, existing decision diagrams, including TDDs, do not leverage such tensor isomorphisms, leaving room for further compression.

A novel approach for representing quantum states has been implemented in Local Invertible Map Decision Diagrams (LIMDD) [18], [19]. By establishing isomorphic relations and extracting local Pauli operators between quantum states, LIMDD achieves superior compression efficiency. Notably, it can represent any stabilizer state using at most n nodes, where n is the number of qubits. In the best-case scenario, LIMDD has been shown to be exponentially more compact than QMDD. However, LIMDD is specifically designed for quantum state representations and cannot be directly applied to general tensor representations or quantum circuit functionality computation.

Emails: hongxin@ios.ac.cn, dac22@mails.tsinghua.edu.cn, gaodc@ios.ac.cn, sanjiang.li@uts.edu.au, jizhengfeng@tsinghua.edu.cn, mingsheng.ying@uts.edu.au

Work partially supported by xxx .

This paper aims to incorporate isomorphic tensor compression into a decision diagram framework. To achieve this, we propose integrating Local Invertible Maps (LIMs) [18] into TDDs, creating a versatile decision diagram that applies to tensor network tasks while maintaining at least the same compression efficiency as TDD. However, integrating LIMs into TDD presents several key challenges:

- 1) **Efficiently identifying and utilizing tensor isomorphisms:** While the concept of tensor isomorphism is straightforward to define (Fig. 1), recognizing and applying these transformations within a decision diagram remains nontrivial. A structured approach is required to detect and exploit isomorphic structures while ensuring TDD's operational efficiency is maintained.
- 2) **Extending beyond Pauli-based equivalences:** LIMDDs rely on Pauli operators to establish equivalences for quantum states, which limits their ability to represent general tensors. A more expressive operator group is needed to enhance compression efficiency and extend applicability beyond simulating quantum states.
- 3) **Ensuring a canonical and compact representation:** Ensuring a canonical and compact representation demands a systematic approach to normalizing tensor structures, which involves refining weight normalization techniques and leveraging efficient tensor transformation algorithms.

To address these challenges, we introduce the Local Invertible Map Tensor Decision Diagram (LimTDD), an extension of TDD that incorporates LIMs for enhanced compression. Our main contributions include:

- 1) Addressing Challenge 1, we formalize tensor vectorization and establish a framework for identifying and utilizing tensor isomorphisms, enabling more effective compression while reserving computational efficiency.
- 2) Addressing Challenge 2, we utilize the XP-stabilizer group [21] in LimTDD, extending its applicability beyond quantum states and improving compression efficiency compared to Pauli-based LIMDD.
- 3) Addressing Challenge 3, we develop optimized algorithms for normalization, slicing, addition, and contraction, enabling efficient computation of quantum circuit functionality and tensor network contraction.
- 4) Additionally, we provide a theoretical comparison of LimTDD with existing decision diagrams and conduct extensive experiments demonstrating its advantages in compactness and computational efficiency for quantum circuit simulation and functionality computation.

The remainder of this paper is structured as follows. Section II provides background on quantum computing, tensor networks, and decision diagrams (TDD and LIMDD). Section III introduces the formal definition of LimTDD, along with its mathematical foundations. Section IV describes key tensor operations within LimTDD, including slicing, addition, and contraction. Section V presents a theoretical comparison between LimTDD, TDD, and LIMDD, analyzing their compression efficiency. Section VI introduces potential applications of LimTDD. Section VII provides experimental results, demonstrating LimTDD's advantages in quantum

$$\begin{array}{l}
 X \text{ gate : } \begin{array}{c} \text{---} \boxed{X} \text{---} \end{array} \quad \begin{bmatrix} 0 & 1 \\ 1 & 0 \end{bmatrix} \\
 P \text{ gate : } \begin{array}{c} \text{---} \boxed{P} \text{---} \end{array} \quad \begin{bmatrix} 1 & 0 \\ 0 & \omega^2 \end{bmatrix} \\
 CZ \text{ gate : } \begin{array}{c} \text{---} \bullet \text{---} \\ | \\ \text{---} \boxed{Z} \text{---} \end{array} \quad \begin{bmatrix} 1 & 0 & 0 & 0 \\ 0 & 1 & 0 & 0 \\ 0 & 0 & 1 & 0 \\ 0 & 0 & 0 & -1 \end{bmatrix}
 \end{array}$$

Fig. 2. Matrix representations of X , P , and CZ gates. Here, ω is an N -th root of the unity $\omega = e^{2\pi i/N}$. To emphasize the degree of the root of the unity, we also denote it as P_N . If not specified, $\omega = e^{2\pi i/16}$.

circuit simulation and tensor network computations. Finally, Section VIII concludes the paper.

II. BACKGROUND

A. Quantum Computing

Quantum computing leverages principles of quantum mechanics to perform computations that classical computers cannot efficiently handle. The fundamental unit of quantum information is the *qubit*, which differs from a classical bit by existing in a superposition of states. A single-qubit state is generally represented as:

$$|\varphi\rangle := \alpha_0 |0\rangle + \alpha_1 |1\rangle, \quad (1)$$

where α_0, α_1 are complex amplitudes satisfying $|\alpha_0|^2 + |\alpha_1|^2 = 1$. Alternatively, a single-qubit state can be represented as a column vector $[\alpha_0, \alpha_1]^\top$ (where \top denotes the transpose). In general, an n -qubit quantum state can be expressed as a 2^n -dimensional vector $[\alpha_0, \alpha_1, \dots, \alpha_{2^n-1}]^\top$ in Hilbert space.

Quantum computation is performed using quantum gates, which are represented by unitary matrices acting on qubits. Common quantum gates include the Pauli gates (X , Y , Z), the Hadamard gate (H), and controlled operations such as the Controlled Z (CZ) gate and the Controlled Not (CNOT) gate (cf. [11]). Each quantum gate has a unique unitary matrix representation in a predefined orthonormal basis, see Fig. 2 for some illustrations. Of particular importance to this paper is the Phase gate P , which is defined with a parameter ω . When $\omega = e^{2\pi i/16}$, the gate P corresponds to the T gate, P^2 corresponds to the S gate, and P^4 corresponds to the Z gate.

The outcome of applying a quantum gate to an input state is determined by multiplying the corresponding unitary matrix with the vector representing the input quantum state. For instance, the result of applying an X gate to the input state $[\alpha_0, \alpha_1]^\top$ is given by $[\alpha_1, \alpha_0]^\top$. In a broader context, an n -qubit quantum gate is represented by a $2^n \times 2^n$ -dimensional unitary transformation matrix.

A quantum circuit is composed of qubits and a sequence of quantum gates. When a quantum circuit operates on an input state, the quantum gates are applied sequentially to the input state. The functionality of an n -qubit quantum circuit can also be described by a $2^n \times 2^n$ -dimensional unitary transformation matrix.

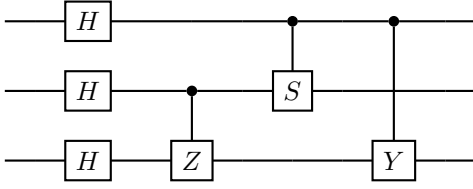


Fig. 3. A quantum circuit with 3 qubits and 6 gates.

Example 1. Consider the circuit shown in Fig. 3. This circuit consists of 3 Hadamard gates, a controlled-Z gate, a controlled-S gate, and a controlled-Y gate. Starting from the input state $|000\rangle$, the output state of this circuit is $\frac{1}{2\sqrt{2}}(|000\rangle + |001\rangle + |010\rangle - |011\rangle - i|100\rangle + i|101\rangle - |110\rangle - |111\rangle)$.

B. Tensors and Tensor Networks

A *tensor* is a multidimensional array associated with a set of indices. In quantum computing, we assume each index takes a value in $\{0, 1\}$. A tensor with an index set $S = \{x_n, \dots, x_1\}$ can be viewed as a mapping $\phi : \{0, 1\}^S \rightarrow \mathbb{C}$, where \mathbb{C} represents the field of complex numbers. For clarity, we denote such a tensor as $\phi_{x_n \dots x_1}$ or $\phi_{\vec{x}}$, and its value on the evaluation $\{x_i \mapsto a_i, 1 \leq i \leq n\}$ as $\phi_{x_n \dots x_1}(a_n, \dots, a_1)$, or simply $\phi_{\vec{x}}(\vec{a})$ or even $\phi(\vec{a})$ when unambiguous. The *rank* of a tensor refers to the number n of its indices. Scalars, 2-dimensional vectors, and 2×2 matrices are considered as rank 0, rank 1, and rank 2 tensors, respectively. An n -qubit quantum state can be regarded as a tensor with n indices.

The primary operation between tensors is *contraction*. Given tensors $\gamma_{\vec{x}, \vec{z}}$ and $\xi_{\vec{y}, \vec{z}}$ sharing a common index set \vec{z} , their contraction results in a new tensor $\phi_{\vec{x}, \vec{y}}$ defined as:

$$\phi_{\vec{x}, \vec{y}}(\vec{a}, \vec{b}) = \sum_{\vec{c} \in \{0, 1\}^{\vec{z}}} \gamma_{\vec{x}, \vec{z}}(\vec{a}, \vec{c}) \cdot \xi_{\vec{y}, \vec{z}}(\vec{b}, \vec{c}). \quad (2)$$

Another useful operation is *slicing*, analogous to the cofactor operation for Boolean functions. For a tensor ϕ with index set $S = \{x, x_n, \dots, x_1\}$, the slicing with respect to $x = c$ (where $c \in \{0, 1\}$) is a tensor $\phi_{x=c}$ over $S' = \{x_n, \dots, x_1\}$ given by:

$$\phi_{x=c}(\vec{a}) := \phi(c, \vec{a}) \quad (3)$$

for any $\vec{a} \in \{0, 1\}^n$. The *negative* and *positive* slicings of ϕ with respect to x are denoted as $\phi_{x=0}$ and $\phi_{x=1}$, respectively.

A *tensor network* is represented by an undirected graph $G = (V, E)$ with zero or multiple open edges, where each vertex v in V represents a tensor, and each edge corresponds to a shared index between two adjacent tensors. By contracting connected tensors (i.e., vertices in V) in an arbitrary order, we obtain a rank m tensor, where m is the number of open edges of G . This tensor, which is independent of the contraction order, is called the tensor representation of the tensor network. For further details, see [9] and [2].

Quantum circuits are natural examples of tensor networks.

Example 2. The circuit shown in Fig. 3 can be represented as a tensor network consisting of three rank 2 tensors and three rank 4 tensors. Contracting these tensors with a tensor

representing the input state $|000\rangle$ yields the following tensor, which represents the output state as shown in Example 1.

$x_3 x_2 x_1$	000	001	010	011	100	101	110	111
ϕ	$\frac{1}{2\sqrt{2}}$	$\frac{1}{2\sqrt{2}}$	$\frac{1}{2\sqrt{2}}$	$\frac{-1}{2\sqrt{2}}$	$\frac{-i}{2\sqrt{2}}$	$\frac{i}{2\sqrt{2}}$	$\frac{-1}{2\sqrt{2}}$	$\frac{-1}{2\sqrt{2}}$

C. TDD for Tensor Network Representation

TDD is a data structure designed to represent and manipulate tensors in a compact and efficient manner. Its core concept involves using a binary branching structure to map data elements to different paths, thereby enabling the compression of repeated data by sharing common branches. The formal definition is as follows:

Definition 1 (Tensor Decision Diagram). A Tensor Decision Diagram (TDD) \mathcal{F} over a set of indices S is a rooted, weighted, and directed acyclic graph $\mathcal{F} = (V, E, \text{idx}, \text{val}, \text{low}, \text{high}, \text{wt})$ defined as follows:

- V is a finite set of nodes which is partitioned into non-terminal nodes V_{NT} and a terminal node v_T . Denote by $r_{\mathcal{F}}$ the unique root node of \mathcal{F} ;
- $\text{idx} : V_{NT} \rightarrow S$ assigns each non-terminal node an index in S ;
- $\text{val} : \{v_T\} \rightarrow \mathbb{C}$ assigns the terminal node a complex value;
- both low and high are mappings in $V_{NT} \rightarrow V$, which assign each non-terminal node with its 0- and 1-successors, respectively;
- $E = \{(v, \text{low}(v)), (v, \text{high}(v)) : v \in V_{NT}\}$ is the set of edges, where $(v, \text{low}(v))$ and $(v, \text{high}(v))$ are called the low- and high-edges of v , respectively. For simplicity, we also assume the root node $r_{\mathcal{F}}$ has a unique incoming edge, denoted e_r , which has no source node;
- $\text{wt} : E \rightarrow \mathbb{C}$ assigns each edge a complex weight. In particular, $\text{wt}(e_r)$ is called the weight of \mathcal{F} , denoted $w_{\mathcal{F}}$.

Each node v of a TDD \mathcal{F} corresponds to a tensor $\Phi(v)$. If v is the terminal node, then $\Phi(v) := \text{val}(v)$ is a rank 0 tensor, i.e., a constant; if v is a non-terminal node, then

$$\Phi(v) := w_0 \cdot \bar{x}_v \cdot \Phi(\text{low}(v)) + w_1 \cdot x_v \cdot \Phi(\text{high}(v)), \quad (4)$$

where $x_v = \text{idx}(v)$, and w_0 and w_1 are the weights on the low- and high-edges of v , respectively. The tensor represented by \mathcal{F} itself is defined to be

$$\Phi(\mathcal{F}) := w_{\mathcal{F}} \cdot \Phi(r_{\mathcal{F}}). \quad (5)$$

Example 3. Fig. 4 (a) gives the TDD representation of the tensor shown in Example 2, where dotted red lines represent the low edges and solid blue lines represent the high edges. The value of the tensor can be obtained by multiplying the weights along the paths. For example, the leftmost path gives the value $\phi_{x_3 x_2 x_1}(000) = \frac{1}{2\sqrt{2}} \times 1 \times 1 \times 1 = \frac{1}{2\sqrt{2}}$. Note that the weight 1 is omitted in the figure.

D. LIMDD for Quantum State Representation

While TDD and QMDD can represent quantum states, LIMDD [18] provides a more compact representation. In this

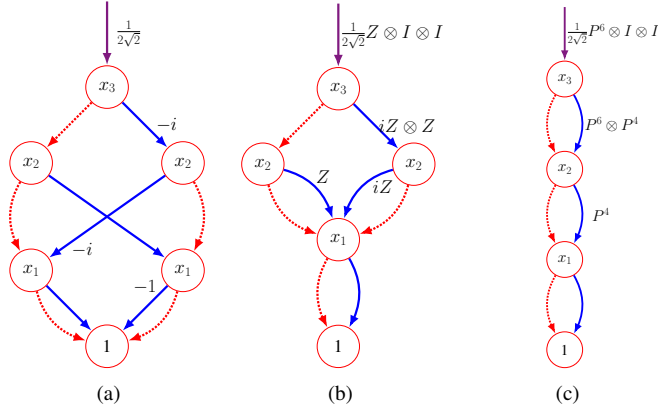


Fig. 4. The TDD (a), LIMDD (b), and LimTDD (c) representations of the output state resulting from simulating the circuit shown in Fig. 3 with input state $|000\rangle$.

framework, two quantum states that differ solely by a local invertible transformation are allowed to share the same node.

Definition 2 (LIM, Quantum State Isomorphism). An n -qubit Local Invertible Map (LIM) is an operator O of the form

$$O = \lambda O_n \otimes \cdots \otimes O_1, \quad (6)$$

where each O_i is an invertible 2×2 matrix and $\lambda \in \mathbb{C}$. The set of all such maps is denoted as $\mathcal{O}(n)$, and the set of all LIMs is defined as

$$\mathcal{O} = \bigcup_{n \in \mathbb{N}} \mathcal{O}(n). \quad (7)$$

Two n -qubit quantum states $|\Phi\rangle$ and $|\Psi\rangle$ are said to be isomorphic if $|\Phi\rangle = O|\Psi\rangle$ for some $O \in \mathcal{O}(n)$.

With the notion of quantum state isomorphism in place, we now introduce Local Invertible Map Decision Diagrams.

Definition 3 (LIMDD). Let \mathcal{G} be a subgroup of \mathcal{O} . An n -qubit \mathcal{G} -LIMDD is a rooted, directed acyclic graph (DAG) that represents an n -qubit quantum state. Formally, a LIMDD is a 6-tuple $(V, E, idx, low, high, wt)$ where:

- V is a finite set of nodes, consisting of non-terminal nodes V_{NT} and a terminal node v_T labelled with integer 1;
- $idx: V_{NT} \rightarrow [n]$ assigns each node a qubit indices in $[n]$;
- low and $high$ are mappings in $V_{NT} \rightarrow V$ that assign each non-terminal node its 0-successor and 1-successor, respectively;
- $E = \{(v, low(v)), (v, high(v)) : v \in V_{NT}\}$ is the set of edges, where $(v, low(v))$ and $(v, high(v))$ are called the low-edge and high-edge of v , respectively. For simplicity, we assume the root node $r_{\mathcal{F}}$ has a unique incoming edge, denoted e_r , which has no source node;
- $wt: E \rightarrow \mathcal{G}$ is a function that labels edges with LIMs.

By overloading the Dirac notation, the semantics of the terminal node is defined to be $|v_T\rangle = 1$, the semantics of an

edge e , directing to a node v , is defined to be

$$|e\rangle = w(e) \cdot |v\rangle,$$

and the semantics of a non-terminal node v is defined to be

$$|v\rangle = |0\rangle \otimes |(v, low(v))\rangle + |1\rangle \otimes |(v, high(v))\rangle.$$

In the framework of [18] and the implementation of [19], the group \mathcal{G} is typically chosen as the stabilizer group. By leveraging isomorphisms among quantum states, LIMDDs achieve greater compactness than QMDDs and TDDs in representing quantum states.

Example 4. Fig. 4 (b) gives the LIMDD representation of the 3-qubit quantum state shown in Example 1. Note that

$$\begin{aligned} & \frac{1}{2\sqrt{2}} (|000\rangle + |001\rangle + |010\rangle - |011\rangle \\ & \quad - i|100\rangle + i|101\rangle - |110\rangle - |111\rangle) \\ & = \frac{1}{2\sqrt{2}} ((|00\rangle - |11\rangle)|+\rangle + (|01\rangle - i|10\rangle)|-\rangle). \end{aligned}$$

Since $|-\rangle = Z|+\rangle$, the two nodes labelled with index x_1 in Fig. 4 (a), representing the state $|+\rangle$ and $|-\rangle$, are merged. The weight has been modified to account for the corresponding Z operator.

The amplitudes of a quantum state can be obtained by multiplying the complex weights along the paths in its LIMDD. However, two important rules must be observed:

- 1) A minus sign must be added if when calculating the amplitude for a $|1\rangle$ state if a Z operator is applied.
- 2) The two branches must be interchanged if an X operator is applied.

We illustrate the first rule with an example.

Example 5. The amplitude of $|011\rangle$ can be calculated by multiplying the complex weights $\frac{1}{2\sqrt{2}} \times 1 \times 1 \times 1$ along the incoming-red-blue-blue path in Fig. 4 (b). A minus sign must be applied because a Z operator is applied to the last qubit when the second qubit is $|1\rangle$.

III. LIMTDD

While LIMDD excels in efficiently representing quantum states, it is limited in its ability to represent and manipulate general tensors. On the other hand, TDD can represent arbitrary tensors but suffers from relatively lower efficiency. In this section, we introduce LimTDD, a novel approach that integrates the strengths of both LIMDD and TDD. By combining their respective advantages, LimTDD not only retains the ability to represent arbitrary tensors but also achieves greater compactness, offering enhanced efficiency and broader applicability.

A. Isomorphism Between Tensors

To effectively represent tensors using LimTDD, we first characterize tensor isomorphism by introducing tensor vectorization. Let \mathcal{G} be a subgroup of \mathcal{O} . As illustrated in Fig. 1, two tensors are considered \mathcal{G} -isomorphic if they differ only by a global coefficient and a local invertible transformation $O \in \mathcal{G}$.

In order to express this isomorphic relation more conveniently and concisely, we introduce the notion of tensor vectorisation:

Definition 4 (Tensor Vectorisation). *Let $\phi_{x_n \dots x_1}$ be a tensor with n indices. Its vectorisation, denoted as $|\phi_{x_n \dots x_1}\rangle\rangle$, is a 2^n -dimensional vector whose i -th element is $\phi(i_n, \dots, i_1)$, where $i_n \dots i_1$ is the binary expansion of the integer i .*

The isomorphism between two tensors can be characterized as follows:

Fact 1. *Two rank n tensors $\phi_{x_n \dots x_1}$ and $\psi_{x_n \dots x_1}$ are \mathcal{G} -isomorphic if and only if there exists $O = \lambda \cdot O_n \otimes \dots \otimes O_1 \in \mathcal{G}$ such that $|\phi_{x_n \dots x_1}\rangle\rangle = \lambda \cdot O_n \otimes \dots \otimes O_1 |\psi_{x_n \dots x_1}\rangle\rangle$.*

This is because, apart from a global coefficient, applying $\lambda \cdot O_n \otimes \dots \otimes O_1$ to $|\psi_{x_n \dots x_1}\rangle\rangle$ is equivalent to contracting an operator O_i over each index x_i of ψ . The key point is to ensure that the indices of both tensors remain aligned.

With this characterization, when computing the decision diagram for a tensor ϕ , we can use the decision diagram representation of ψ and assign a weight $\lambda \cdot O_n \otimes \dots \otimes O_1$ to its incoming edge. This process can be recursively applied to the sub-tensors $\psi_{x_n=0}$ and $\psi_{x_n=1}$.

Example 6. *Consider the 2-qubit sub-circuit composed of two H gates and the CZ gate of the circuit shown in Fig. 3. Let x_2 and x_1 denote the indices corresponding to the input of the two qubits, and y_2 and y_1 denote the indices corresponding to their outputs, respectively. Let $\phi_{y_2 x_2 y_1 x_1}$ represent the corresponding tensor. Its vectorization is the vector given in Table I.*

Note that the vectorisation of $\phi_{y_2=0}$, corresponding to the first half of the vector, is $|\phi_{y_2=0}\rangle\rangle = \frac{1}{2}[1, 1, 1, -1, 1, 1, 1, -1]^T$, and the vectorisation of $\phi_{y_2=1}$, corresponding to the second half of the vector, is $|\phi_{y_2=1}\rangle\rangle = \frac{1}{2}[1, 1, -1, 1, -1, -1, 1, -1]^T$. Because $|\phi_{y_2=1}\rangle\rangle = Z \otimes Z \otimes I \cdot |\phi_{y_2=0}\rangle\rangle$, the two sub-tensors are isomorphic.

Let $O = \lambda \cdot O_n \otimes \dots \otimes O_1$. We define the following notations:

- $c(O) = \lambda$,
- $O[i] = O_i$ for $1 \leq i \leq n$,
- $O[i] = O_i \otimes \dots \otimes O_1$ for $1 \leq i \leq n$.

Suppose $\lambda = r \cdot e^{2\pi i \theta}$ for some real number $r \in \mathbb{R}$. We call θ the angle of λ , denoted as $\text{ang}(\lambda) = \theta$.

In the remainder of this paper, when there is no ambiguity, we will not distinguish between $\phi_{x_n \dots x_1}$ and $|\phi_{x_n \dots x_1}\rangle\rangle$. Additionally, we will use the notations $\lambda \cdot \phi_{x_n \dots x_1}$ and $O \cdot \phi_{x_n \dots x_1}$ to represent multiplying a tensor by a scalar or contracting an operator on corresponding indices.

B. LimTDD: Definition and Examples

Definition 5 (LimTDD). *Let \mathcal{G} be a subgroup of \mathcal{O} . A \mathcal{G} -LimTDD \mathcal{F} over a set of indices S is a rooted, weighted, and directed acyclic graph $\mathcal{F} = (V, E, \text{id}_x, \text{low}, \text{high}, \text{wt})$ defined as follows:*

- V is a finite set of nodes which consists of non-terminal nodes V_{NT} and a terminal node v_T labelled with integer 1. Denote by $r_{\mathcal{F}}$ the unique root node of \mathcal{F} ;
- $\text{id}_x : V_{NT} \rightarrow S$ assigns each non-terminal node an index in S . We call $\text{id}_x(r_{\mathcal{F}})$ the top index of \mathcal{F} , if $r_{\mathcal{F}}$ is not the terminal node;

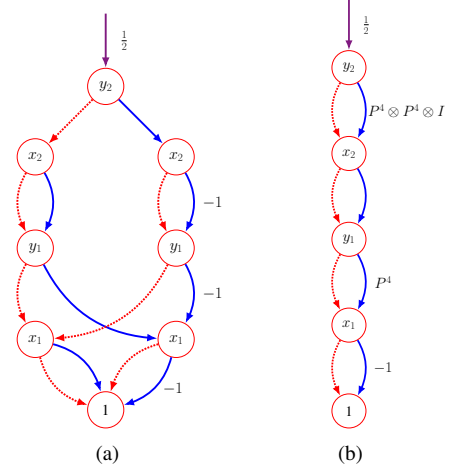


Fig. 5. The TDD and LimTDD representations of the tensor shown in Example 6.

- both low and high are mappings in $V_{NT} \rightarrow V$, which assign each non-terminal node with its 0- and 1-successors, respectively;
- $E = \{(v, \text{low}(v)), (v, \text{high}(v)) : v \in V_{NT}\}$ is the set of edges, where $(v, \text{low}(v))$ and $(v, \text{high}(v))$ are called the low- and high-edges of v , respectively. For simplicity, we also assume the root node $r_{\mathcal{F}}$ has a unique incoming edge, denoted e_r , which has no source node;
- $\text{wt} : E \rightarrow \mathcal{G}$ assigns each edge a weight in \mathcal{G} . $\text{wt}(e_r)$ is called the weight of \mathcal{F} , and denoted $w_{\mathcal{F}}$.

For any edge e connected to a node v , the tensor represented by e is defined as $\Phi(e) = \text{wt}(e) \cdot |\Phi(v)\rangle\rangle$, where for any internal node v with index x_v ,

$$\Phi(v) = \bar{x}_v \cdot \Phi((v, \text{low}(v))) + x_v \cdot \Phi((v, \text{high}(v))), \quad (8)$$

and the terminal node represents the scalar 1.

In this paper, for a rank n tensor with indices x_n, \dots, x_1 , we always adopt the ordering $x_n < \dots < x_1$ for simplicity. This means x_n is above x_1 in the representation of LimTDD. In practical implementations, we choose \mathcal{G} to be the XP-Stabilizer group [21], which will be introduced in the following subsection.

We next provide two examples to illustrate the construction of LimTDD.

Example 7. *Fig. 5 illustrates the TDD and LimTDD representations of the tensor $\phi_{y_2 x_2 y_1 x_1}$ from Example 6. The TDD representation consists of 8 nodes, while the LimTDD representation requires only 5 nodes. Notably, the high edge of the root node in the LimTDD representation carries the operator $P^4 \otimes P^4 \otimes I$, which corresponds to the relationship $|\phi_{y_2=1}\rangle\rangle = Z \otimes Z \otimes I \cdot |\phi_{y_2=0}\rangle\rangle$ shown in Example 6. Similarly, the operator P^4 on the high edge of the y_0 node reflects the relationship $|\phi_{y_2 x_2 y_1=001}\rangle\rangle = Z \cdot |\phi_{y_2 x_2 y_1=000}\rangle\rangle$.*

Additionally, LimTDD can represent quantum states, as quantum states can also be viewed as tensors.

TABLE I
THE VECTORIZATION OF THE TENSOR $\phi_{y_2x_2y_1x_1}$ IN EXAMPLE 6.

$y_2x_2y_1x_1$	0000	0001	0010	0011	0100	0101	0110	0111	1000	1001	1010	1011	1100	1101	1110	1111
ϕ	$\frac{1}{2}$	$\frac{1}{2}$	$\frac{1}{2}$	$-\frac{1}{2}$	$\frac{1}{2}$	$\frac{1}{2}$	$\frac{1}{2}$	$-\frac{1}{2}$	$\frac{1}{2}$	$\frac{1}{2}$	$-\frac{1}{2}$	$\frac{1}{2}$	$-\frac{1}{2}$	$-\frac{1}{2}$	$\frac{1}{2}$	$-\frac{1}{2}$

Example 8. Fig. 4 (c) shows the LimTDD representation of the tensor $\phi_{x_3x_2x_1}$ from Example 2. The node labelled with index x_3 represents the tensor $\psi_{x_3x_2x_1} = [1, 1, 1, -1, 1, -1, -i, i]^T$. Since $|\phi_{x_3x_2x_1}\rangle\rangle = \frac{1}{2\sqrt{2}}P^6 \otimes I \otimes I|\psi_{x_3x_2x_1}\rangle\rangle$, the weight $\frac{1}{2\sqrt{2}}P^6 \otimes I \otimes I$ is shown on the incoming edge of the LimTDD representation. The weight $P^6 \otimes P^4$ indicates that $|\psi_{x_3=1}\rangle\rangle = P^6 \otimes P^4|\psi_{x_3=0}\rangle\rangle$, and the weight P^4 implies that $|\psi_{x_3x_2=01}\rangle\rangle = P^4|\psi_{x_3x_2=00}\rangle\rangle$.

Typically, a node in a LimTDD is uniquely determined by its index, its two successors, and the weights on the two edges connecting to those successors, denoted as

$$\left(v_0 \xleftarrow{w_0} v \xrightarrow{w_1} v_1 \right).$$

Similarly, a LimTDD is uniquely determined by its root node and the weight on the incoming edge, represented as:

$$\left(w_{\mathcal{F}}, \left(v_0 \xleftarrow{w_0} v \xrightarrow{w_1} v_1 \right) \right),$$

or simply as

$$\xrightarrow{w_{\mathcal{F}}} \left(v \right).$$

It is worth noting that when the group \mathcal{G} is restricted to Pauli group, LimTDD is equivalent to LIMDD representing quantum states, and when \mathcal{G} is restricted to the scalar multiples of the identity (i.e., $\mathcal{G} \subset \mathbb{C} \cdot I$), LimTDD reduces exactly to standard TDD.

C. XP-Operators

While the definition of tensor isomorphism allows for general 2×2 invertible maps O_i , in practice, the operators are restricted to a smaller group for computational efficiency. For LIMDD, this group is restricted to Pauli operators, as their algebraic properties simplify representation and computation.

In this subsection, we extend these operators using XP-operators [21]. This extension allows for more compact decision diagrams while leveraging the algebraic properties of XP-operators to ensure canonicity. The basic notations and results of this subsection come from [21].

An n -qubit XP-operator of precision N (where $\omega = e^{2\pi i/N}$) is an operator of the form:

$$XP_N(p|\mathbf{x}|\mathbf{z}) := \omega^p \bigotimes_{0 \leq i < n} X^{\mathbf{x}[i]} P^{\mathbf{z}[i]}, \quad (9)$$

where p , $\mathbf{x}[i]$, and $\mathbf{z}[i]$ are integers satisfying:

- $0 \leq p < 2N$,
- $0 \leq \mathbf{x}[i] < 2$,
- $0 \leq \mathbf{z}[i] < N$.

We call p , \mathbf{x} , and \mathbf{z} the phase component, X -component, and Z -component of the XP-operator, respectively. It is easy to see

that two XP-operators $XP_N(p|\mathbf{x}|\mathbf{z})$ and $XP_N(p'|\mathbf{x}'|\mathbf{z}')$ are identical if and only if $p = p'$, $\mathbf{x} = \mathbf{x}'$, and $\mathbf{z} = \mathbf{z}'$.

As established in [21, Proposition 4.1], XP-operators possess useful group properties. Examples include elegant characterizations of the unit operator, multiplication, and inverses of XP-operators (cf. VIII-A). Of particular importance is the following result: Let $G = \{g_1, \dots, g_m\}$ be a set of XP-operators, and denote the group generated by G as $\langle G \rangle$. It was shown in [21] that there exists a unique set of diagonal operators $S_Z := \{B_j : 0 \leq j < s\}$ and non-diagonal operators $S_X := \{A_i : 0 \leq i < r\}$, called the *canonical generators* of $\langle G \rangle$, such that all group elements $g \in \langle G \rangle$ can be expressed as $g = S_X^{\mathbf{a}} S_Z^{\mathbf{b}}$, where $\mathbf{a} \in \mathbb{Z}_2^{|\mathcal{S}_X|}$ and $\mathbf{b} \in \mathbb{Z}_2^{|\mathcal{S}_Z|}$. Furthermore, two sets of XP-operators of precision N generate the same group if and only if they have the same canonical generators.

D. LimTDD Normalization

In decision diagrams that use weighted paths, the functionality represented is determined by multiplying the weights along those paths. This can lead to a situation where different decision diagrams, with different weight assignments, represent the same underlying functionality. Normalization is a process that reduces this ambiguity, aiming to create a canonical representation where each functionality has a unique diagram representation. For LimTDD, as the weight on an edge can be a LIM, the normalization process is more complicated than TDD.

Lemma 1. Suppose v is an internal node in a LimTDD, $v_0 = \text{low}(v)$ and $v_1 = \text{high}(v)$ its child nodes, and w_0, w_1 the weights on the low- and high-edges of v , respectively. Let g_i be any stabilizer of $|v_i\rangle\rangle$ ($i = 0, 1$) and $0 \leq k < N$. The following LimTDDs

$$\begin{aligned} & \left(1, \left(v_0 \xleftarrow{w_0 \cdot g_0} v \xrightarrow{w_1 \cdot g_1} v_1 \right) \right), \\ & \left(P^k \otimes (w_0 \cdot g_0), \left(v_0 \xleftarrow{I} v \xrightarrow{\omega^{-2k} \cdot g_0^\dagger \cdot w_0^\dagger \cdot w_1 \cdot g_1} v_1 \right) \right), \\ & \left(X \otimes (w_1 \cdot g_1), \left(v_1 \xleftarrow{I} v \xrightarrow{g_1^\dagger \cdot w_1^\dagger \cdot w_0 \cdot g_0} v_0 \right) \right) \end{aligned}$$

represent the same tensor as

$$\left(1, \left(v_0 \xleftarrow{w_0} v \xrightarrow{w_1} v_1 \right) \right).$$

The above lemma shows that there are many different LimTDD representations of the same tensor. To select a unique representation, we adopt the following assumptions: For two nodes v_1, v_2 , $v_1 < v_2$ if v_1 is created before v_2 (normally with a smaller id). For two weights $w_1 = r_1 e^{2\pi i \theta_1} XP_N(p_1|\mathbf{x}_1|\mathbf{z}_1)$ and $w_2 = r_2 e^{2\pi i \theta_2} XP_N(p_2|\mathbf{x}_2|\mathbf{z}_2)$, $w_1 < w_2$ if $(\mathbf{x}_1|\mathbf{z}_1|r_1|\theta_1|p_1) < (\mathbf{x}_2|\mathbf{z}_2|r_2|\theta_2|p_2)$ in the

lexicographical order. Here, $r_1, r_2, \theta_1, \theta_2 \in \mathbb{R}$, and $r_1, r_2 \geq 0$, $0 \leq \theta_1, \theta_2 < \text{ang}(\omega)$.

For any node v in a LimTDD, we write

$$\text{Stab}(v) = \{O \in \mathcal{O} \mid O|\Phi(v)\rangle\rangle = |\Phi(v)\rangle\rangle\}. \quad (10)$$

The procedure for calculating $\text{Stab}(v)$ is described in VIII-B. There are two sets of weights that are important:

$$W_0 := \{g_0^\dagger \cdot w_0^\dagger \cdot w_1 \cdot g_1 \mid g_0 \in \text{Stab}(v_0), g_1 \in \text{Stab}(v_1)\},$$

$$W_1 := \{g_1^\dagger \cdot w_1^\dagger \cdot w_0 \cdot g_0 \mid g_0 \in \text{Stab}(v_0), g_1 \in \text{Stab}(v_1)\}.$$

For LimTDD, the normalization process incorporates the following three principles for each internal node v to make this representation unique:

- 1) $\text{low}(v) \leq \text{high}(v)$.
- 2) $\text{wt}((v, \text{low}(v))) = I$, unless it is 0.
- 3) If $\text{low}(v) < \text{high}(v)$, then $\text{wt}((v, \text{high}(v)))$ is the smallest one in W_1 ; otherwise, $\text{low}(v) = \text{high}(v)$ and $\text{wt}((v, \text{high}(v)))$ is the smallest in $W_0 \cup W_1$.

The normalization process adopts a bottom-up approach and enforces the three conditions to every node using a `loc_norm` procedure (cf. Algorithm 1). Suppose v_0 and v_1 are the root nodes of the two sub-LimTDDs, \mathcal{F}_0 and \mathcal{F}_1 , that are subjected to the normalization procedure and v is their intended parent node with index x . Let $v_i = r_{\mathcal{F}_i}$ be the root node of \mathcal{F}_i for $i = 0, 1$. We need to decide which of v_0 and v_1 should be the 0-successor of v , and determine the normalized weights on the low and high edges of v .

Without loss of generality, we assume $v_0 \leq v_1$.¹ If $v_0 < v_1$, i.e., v_0 is created before v_1 , we set $\text{low}(v) = v_0$ and $\text{high}(v) = v_1$, and select the smallest value in W_1 as the weight on the high edge; otherwise, $v_0 = v_1$ and we select the smallest value w'_1 in $W_0 \cup W_1$ as the weight on the high edge. After that, the weight of the low-edge will be set to I (unless it is 0), and the weight of the resulting LimTDD will be adjusted correspondingly.

In this algorithm, the subroutine `make_dd(w, x, w_0, v_0, w_1, v_1)` is used to construct a LimTDD with weight w and root node v , where $\text{idx}(v) = x$, $\text{low}(v) = v_0$, $\text{high}(v) = v_1$, $\text{wt}(v, v_0) = w_0$ and $\text{wt}(v, v_1) = w_1$, i.e., $(w, \textcircled{v_0} \xleftarrow{w_0} v \xrightarrow{w_1} \textcircled{v_1})$. In the last step of the procedure, we check if the node of the resulted LimTDD already exists in the `unique_table`; if so, reuse the node; otherwise, we generate a new one and store it on the table with the hash key $(x, w_0, r_{\mathcal{F}_0}, w_1, r_{\mathcal{F}_1})$. With these techniques, we make the LimTDD unique.

New local normalizations can also be obtained from established ones.

Lemma 2. Suppose $\text{loc_norm}(x, \xrightarrow{w_0} \textcircled{v_0}, \xrightarrow{w_1} \textcircled{v_1}) = \xrightarrow{w} \textcircled{v}$. Then we have the following new local normalizations:

- (i) $\text{loc_norm}(x, \xrightarrow{O \cdot w_0} \textcircled{v_0}, \xrightarrow{O \cdot w_1} \textcircled{v_1}) = \xrightarrow{O \cdot w} \textcircled{v}$;
- (ii) $\text{loc_norm}(x, \xrightarrow{w_0} \textcircled{v_0}, \xrightarrow{\omega^{2k} w_1} \textcircled{v_1}) = \xrightarrow{(P^k \otimes I) \cdot w} \textcircled{v}$;
- (iii) $\text{loc_norm}(x, \xrightarrow{w_1} \textcircled{v_1}, \xrightarrow{w_0} \textcircled{v_0}) = \xrightarrow{(X \otimes I) \cdot w} \textcircled{v}$, if $v_0 \neq v_1$ or $w_0 \neq w_1$;

¹If otherwise, we swap the two nodes.

Algorithm 1 `loc_norm($x, \mathcal{F}_0, \mathcal{F}_1$)`

Input: Two normalized LimTDDs \mathcal{F}_i with root v_i and weight w_i ($i = 0, 1$); and an index x . We require $v_0 \leq v_1$.

Output: A normalized LimTDD \mathcal{F} .

```

1:  $b_n = 0$  # Are  $v_0, v_1$  exchanged?
2: if  $w_0 = w_1 = 0$  then
3:   return make_dd(0, x, 0, v_0, 0, v_1) # a DD
   representing the 0 tensor
4: end if
5:  $w_{temp} \leftarrow \min_{g_0 \in \text{Stab}(v_0), g_1 \in \text{Stab}(v_1)} g_0^\dagger \cdot w_0^\dagger \cdot w_1 \cdot g_1$ 
6:  $w_{temp2} \leftarrow \min_{g_0 \in \text{Stab}(v_0), g_1 \in \text{Stab}(v_1)} g_1^\dagger \cdot w_1^\dagger \cdot w_0 \cdot g_0$ 
7: if  $v_1 = v_0$  and  $w_{temp2} < w_{temp}$  then
8:    $b_n \leftarrow 1$ 
9:    $w \leftarrow w_1 \cdot g_1^*$  #  $g_1^*$  is the stabilizer of  $v_1$ 
   which yields  $w_{temp2}$ 
10:   $w'_1 \leftarrow w_{temp2}$ 
11: else
12:   $w \leftarrow w_0 \cdot g_0^*$  #  $g_0^*$  is the stabilizer of  $v_0$ 
   which yields  $w_{temp}$ 
13:   $w'_1 \leftarrow w_{temp}$ 
14: end if
15:  $w'_0 \leftarrow I$ 
16:  $k \leftarrow \lfloor \text{ang}(w_1) / 2\omega \rfloor$ 
17:  $w'_1 \leftarrow w'_1 / \omega^{2k}$ 
18:  $w \leftarrow X^{b_n} P^k \otimes w$ 
19:  $dd \leftarrow \text{make\_dd}(w, x, w'_0, v_0, w'_1, v_1)$ 
20: return check\_unique\_table(dd)

```

- (iv) $\text{loc_norm}(x, \xrightarrow{w_0 \cdot g_0} \textcircled{v_0}, \xrightarrow{w_1 \cdot g_1} \textcircled{v_1}) = \xrightarrow{w} \textcircled{v}$, for any $g_0 \in \text{Stab}(v_0)$ and $g_1 \in \text{Stab}(v_1)$.

IV. ALGORITHMS

This section presents algorithms for constructing LimTDDs from tensors and performing key operations such as addition and contraction. All algorithms are implemented recursively. As with TDDs, we employ local normalization whenever a node is created. Additionally, we use the `computed_table` hash table technique to prevent redundant calculations.

A. LimTDD Generation

To generate the LimTDD representation of a tensor, we recursively generate the LimTDD representations of its two sub-tensors and then apply the normalization procedure. For a scalar, the representation is a LimTDD with a single node (the terminal node) weighted by that scalar.

Algorithm 2 shows the process of generating the LimTDD for a tensor. The construction has a time complexity that is linear in the size of the tensor (i.e., the number of values in the tensor).

B. LimTDD Slicing

Let \mathcal{F} be the LimTDD representation of tensor $\phi_{x_n \dots x_1}$. In this section, we describe how to extract from \mathcal{F} the LimTDDs $\mathcal{F}_{x_i=c}$ that represent the tensors $\phi_{x_i=c}$ for $c \in \{0, 1\}$.

Algorithm 2 *LimTDD_generate*(ϕ)

Input: A tensor ϕ over a linearly ordered index set S .
Output: The normalized LimTDD of ϕ .

- 1: **if** $\phi \equiv c$ is a constant **then**
- 2: **return** $\xrightarrow{c} \textcircled{v_T}$
- 3: **end if**
- 4: $x \leftarrow$ the smallest index of ϕ
- 5: $r_0 \leftarrow \text{LimTDD_generate}(\phi_{x=0})$
- 6: $r_1 \leftarrow \text{LimTDD_generate}(\phi_{x=1})$
- 7: **return** $\text{loc_norm}(x, r_0, r_1)$

First, consider the case when $x_i = x_n$ is the top index. Suppose $\mathcal{F} = \left(w_{\mathcal{F}} \textcircled{v_0} \xleftarrow{w_0} \textcircled{v} \xrightarrow{w_1} \textcircled{v_1} \right)$, with $w_{\mathcal{F}} = X^{b_n} P^{z_n} \otimes w$. Note that P^{z_n} adds a phase ω^{2z_n} to the weight of the high edge, and X^{b_n} swaps the 0-successor and 1-successor if $b_n = 1$. Thus,

- if $b_n = 0$, $\mathcal{F}_{x_i=c} = \xrightarrow{w w_c} \textcircled{v_c}$, and
- if $b_n = 1$, $\mathcal{F}_{x_i=c} = \xrightarrow{w w_{1-c}} \textcircled{v_{1-c}}$.

Here, $w_1 = \omega^{2z_n} w_1$.

If $x_i \neq x_n$ (i.e., x_i is not the top index), we first calculate $\mathcal{F}_{x_n=b}$ for $b \in \{0, 1\}$, then recursively calculate $(\mathcal{F}_{x_n=b})_{x_i=c}$, and combine the results.

Algorithm 3 provides the procedure for slicing. This procedure extracts the portion of data in $\Phi(\mathcal{F})$ with $x_i = c$. This lead to the following lemma:

Lemma 3. *Let \mathcal{F} be the LimTDD of tensor $\phi_{x_n \dots x_1}$ and define $\mathcal{F}_{x_i=c} = \text{Slicing}(\mathcal{F}, x_i, c)$. Then, $\mathcal{F}_{x_i=c}$ is the LimTDD representation of the tensor $\phi_{x_i=c}$ for $c \in \{0, 1\}$.*

Considering the root node of the LimTDD, the Slicing operation is the inverse operation of loc_norm : applying the loc_norm operation to the two sliced sub-LimTDDs with respect to x_n retrieves \mathcal{F} .

Lemma 4. *Let \mathcal{F} be the LimTDD representation of tensor $\phi_{x_n \dots x_1}$. Then $\text{loc_norm}(x_n, \mathcal{F}_{x_n=0}, \mathcal{F}_{x_n=1}) = \mathcal{F}$.*

C. LimTDD Addition

Let \mathcal{F} and \mathcal{G} be two LimTDDs over an index set S . The sum of \mathcal{F} and \mathcal{G} , denoted $\mathcal{F} + \mathcal{G}$, is a LimTDD representing the tensor $\Phi(\mathcal{F}) + \Phi(\mathcal{G})$. Similar to TDD addition, the addition of two LimTDDs can be calculated recursively by adding their sub-LimTDDs. For any $x \in S$ where $x \preceq \text{id}_x(r_{\mathcal{F}})$ and $x \preceq \text{id}_x(r_{\mathcal{G}})$, the LimTDD version of the Boole-Shannon expansion gives us

$$\Phi(\mathcal{F}) + \Phi(\mathcal{G}) = \bar{x} \cdot (\Phi(\mathcal{F}_{x=0}) + \Phi(\mathcal{G}_{x=0})) + x \cdot (\Phi(\mathcal{F}_{x=1}) + \Phi(\mathcal{G}_{x=1})).$$

Here $\mathcal{F}_{x=c}$ and $\mathcal{G}_{x=c}$ are the sub-LimTDDs as defined in Lemma 3 for $c \in \{0, 1\}$.

To improve the efficiency of reusing intermediate results, we first transfer the weights of the two LimTDDs to one of them before performing the recursive step. As illustrated in Fig. 6, to calculate the sum of $O_6 \otimes \dots \otimes O_1 |\phi\rangle\rangle$ and $O_{12} \otimes \dots \otimes O_7 |\psi\rangle\rangle$,

Algorithm 3 *Slicing*(\mathcal{F}, x, c)

Input: A LimTDD \mathcal{F} with weight $w_{\mathcal{F}} = \lambda X^{b_n} P^{z_n} \otimes w$ representing the tensor ϕ ; an index x and a value $c \in \{0, 1\}$.
Output: The sub-LimTDD of \mathcal{F} that represents $\phi_{x=c}$.

- 1: **if** \mathcal{F} is a trivial LimTDD **then**
- 2: **return** \mathcal{F}
- 3: **end if**
- 4: $x' \leftarrow \text{id}_x(r_{\mathcal{F}})$
- 5: **if** $x < x'$ **then**
- 6: **return** \mathcal{F}
- 7: **end if**
- 8: **if** $x = x'$ **then**
- 9: $dd \leftarrow$ an empty LimTDD
- 10: $v_0 \leftarrow \text{low}(r_{\mathcal{F}})$
- 11: $v_1 \leftarrow \text{high}(r_{\mathcal{F}})$
- 12: $w_0 \leftarrow \text{wt}(r_{\mathcal{F}}, \text{low}(r_{\mathcal{F}}))$
- 13: $w_1 \leftarrow \text{wt}(r_{\mathcal{F}}, \text{high}(r_{\mathcal{F}}))$
- 14: **if** $c = 0$ **then**
- 15: $dd.\text{node} = v_{b_n}$
- 16: $dd.\text{weight} = \lambda w w_{b_n} \omega^{2z b_n}$
- 17: **else**
- 18: $dd.\text{node} = v_{1-b_n}$
- 19: $dd.\text{weight} = \lambda w w_{1-b_n} \omega^{2z(1-b_n)}$
- 20: **end if**
- 21: **return** dd
- 22: **end if**
- 23: **if** $x > x'$ **then**
- 24: $r_0 \leftarrow \text{Slicing}(\text{Slicing}(\mathcal{F}, x', 0), x, c)$
- 25: $r_1 \leftarrow \text{Slicing}(\text{Slicing}(\mathcal{F}, x', 1), x, c)$
- 26: **return** $\text{loc_norm}(x', r_0, r_1)$
- 27: **end if**

we first compute $(O_{12} \otimes \dots \otimes O_7)^\dagger \cdot O_6 \otimes \dots \otimes O_1 |\phi\rangle\rangle + |\psi\rangle\rangle$ and then multiply the weight of the result by $O_{12} \otimes \dots \otimes O_7$. This approach allows us to reuse the result when computing two tensors that differ only by a multiplicative factor. For example, when calculating $O \cdot O_6 \otimes \dots \otimes O_1 |\phi\rangle\rangle + O \cdot O_{12} \otimes \dots \otimes O_7 |\psi\rangle\rangle$, the intermediate result can be reused, increasing the computational efficiency. In the algorithm, $\mathcal{F} < \mathcal{G}$ means that $r_{\mathcal{F}} < r_{\mathcal{G}}$ or $r_{\mathcal{F}} = r_{\mathcal{G}}$ and $w_{\mathcal{F}} < w_{\mathcal{G}}$.

Algorithm 4 implements the add operation for LimTDDs, in a node-wise manner.

D. LimTDD Contraction

Contraction is a fundamental operation in tensor networks. This subsection details how to efficiently implement contraction using LimTDDs.

Let \mathcal{F} and \mathcal{G} be two LimTDDs, S the set of indices appearing in \mathcal{F} or \mathcal{G} , and var a subset of S representing the variables to be contracted. We use $\text{cont}(\cdot)$ for both tensor and LimTDD contractions. For any $x \in S$ with $x \preceq \text{id}_x(r_{\mathcal{F}})$ and $x \preceq \text{id}_x(r_{\mathcal{G}})$, Eq. 2 implies that if $x \in \text{var}$, then $\text{cont}((\Phi(\mathcal{F}), \Phi(\mathcal{G}), \text{var}))$ equals

$$\sum_{c=0}^1 \text{cont}(\Phi(\mathcal{F}_{x=c}), \Phi(\mathcal{G}_{x=c}), \text{var} \setminus \{x\});$$

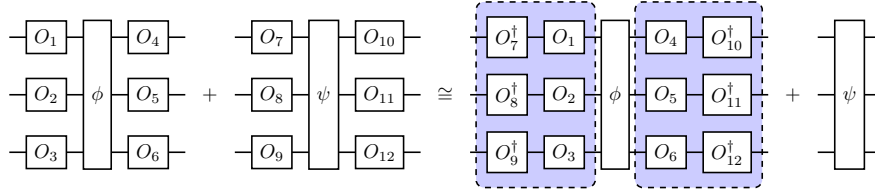
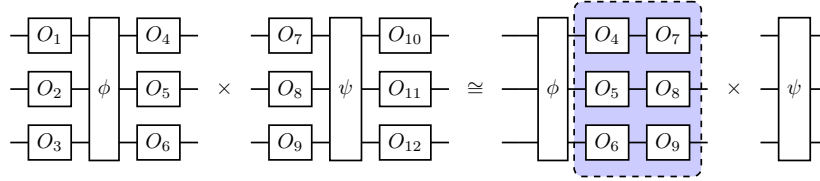


Fig. 6. The addition of two tensors using LimTDD.


 Fig. 7. The contraction of two tensors using LimTDD, where \times denotes tensor contraction.

Algorithm 4 $\text{add}(\mathcal{F}, \mathcal{G})$

Input: Two LimTDDs \mathcal{F} and \mathcal{G} .

Output: The LimTDD representation of $\Phi(\mathcal{F}) + \Phi(\mathcal{G})$.

- 1: **if** $r_{\mathcal{F}} = r_{\mathcal{G}}$ and $\text{wt}(\mathcal{F}) = c \cdot \text{wt}(\mathcal{G})$ **then**
 - 2: $dd \leftarrow \mathcal{F}$
 - 3: $dd.\text{weight} \leftarrow w_{\mathcal{F}} + w_{\mathcal{G}}$
 - 4: **return** dd
 - 5: **end if**
 - 6: $l \leftarrow$ the smaller one of \mathcal{F} and \mathcal{G}
 - 7: $h \leftarrow$ the bigger one of \mathcal{F} and \mathcal{G}
 - 8: $\text{temp}_w \leftarrow \text{wt}(h)$
 - 9: $\text{wt}(l) \leftarrow \text{wt}(h)^\dagger \cdot \text{wt}(l)$
 - 10: $\text{wt}(h) \leftarrow I$
 - 11: $dd \leftarrow \text{find_computed_table}(l, h, +)$
 - 12: **if** dd is empty **then**
 - 13: $x \leftarrow$ the smaller index of $r_{\mathcal{F}}$ and $r_{\mathcal{G}}$
 - 14: $r_0 \leftarrow \text{add}(l_{x=0}, h_{x=0})$
 - 15: $r_1 \leftarrow \text{add}(l_{x=1}, h_{x=1})$
 - 16: $dd \leftarrow \text{loc_norm}(x, r_0, r_1)$
 - 17: **end if**
 - 18: $dd.\text{weight} \leftarrow \text{temp}_w \cdot dd.\text{weight}$
 - 19: **return** dd
-

otherwise, it equals

$$\bar{x} \cdot \text{cont}(\Phi(\mathcal{F}_{x=0}), \Phi(\mathcal{G}_{x=0}), \text{var}) \\ + x \cdot \text{cont}(\Phi(\mathcal{F}_{x=1}), \Phi(\mathcal{G}_{x=1}), \text{var}).$$

This means that calculating the contraction of \mathcal{F} and \mathcal{G} involves calculating the contraction of their sub-LimTDDs and then adding or combining the results.

Algorithm 5 provides the detailed procedure for LimTDD contraction. It's important to note that while LimTDD is generally more compact and efficient than TDD, its worst-case complexity, like TDD, is related to the number of non-zero paths in the two diagrams involved in the operation.

Algorithm 5 $\text{cont}(\mathcal{F}, \mathcal{G}, \text{var})$

Input: Two LimTDDs \mathcal{F} and \mathcal{G} ; the set var of variables to be contracted.

Output: The LimTDD obtained by contracting \mathcal{F} , \mathcal{G} over var .

- 1: **if** both \mathcal{F} and \mathcal{G} are trivial **then**
 - 2: $dd \leftarrow \mathcal{F}$
 - 3: $dd.\text{weight} \leftarrow w_{\mathcal{F}} \cdot w_{\mathcal{G}} \cdot 2^{\text{len}(\text{var})}$
 - 4: **return** dd
 - 5: **end if**
 - 6: $\text{temp}_w =$ uncontracted operators in $\text{wt}(\mathcal{F})$
 - 7: $\text{temp}_w =$ uncontracted operators in $\text{wt}(\mathcal{G})$
 - 8: $\text{wt}(\mathcal{G}) = w(\mathcal{G}) / \text{temp}_w$
 - 9: $\text{wt}(\mathcal{F}) = w(\mathcal{G})^\dagger \cdot \text{wt}(\mathcal{F}) / \text{temp}_w$
 - 10: $\text{wt}(\mathcal{G}) = I$
 - 11: $dd \leftarrow \text{find_computed_table}(\mathcal{F}, \mathcal{G}, \times)$
 - 12: **if** dd is empty **then**
 - 13: **if** \mathcal{G} is identity **then**
 - 14: $dd \leftarrow \mathcal{F}$
 - 15: **else**
 - 16: $x \leftarrow$ the smaller index of $r_{\mathcal{F}}$ and $r_{\mathcal{G}}$
 - 17: **if** $x \in \text{var}$ **then**
 - 18: $r_0 \leftarrow \text{cont}(\mathcal{F}_{x=0}, \mathcal{G}_{x=0}, \text{var} \setminus \{x\})$
 - 19: $r_1 \leftarrow \text{cont}(\mathcal{F}_{x=1}, \mathcal{G}_{x=1}, \text{var} \setminus \{x\})$
 - 20: $dd \leftarrow \text{add}(r_0, r_1)$
 - 21: **else**
 - 22: $r_0 \leftarrow \text{cont}(\mathcal{F}_{x=0}, \mathcal{G}_{x=0}, \text{var})$
 - 23: $r_1 \leftarrow \text{cont}(\mathcal{F}_{x=1}, \mathcal{G}_{x=1}, \text{var})$
 - 24: $dd \leftarrow \text{loc_norm}(x, r_0, r_1)$
 - 25: **end if**
 - 26: **end if**
 - 27: **end if**
 - 28: $dd.\text{weight} = \text{temp}_w \cdot \text{temp}_w \cdot dd.\text{weight}$
 - 29: **return** dd
-

V. COMPACTNESS

In this section, we prove that LimTDD is theoretically more compact than LIMDD and TDD, and we demonstrate that the gap can be exponential in some cases. To this end, we first establish a characterization of isomorphic tensors in terms of their LimTDDs.

Let \mathcal{XP}_N denote the group of XP-Stabilizers with precision N , where $\omega = e^{2\pi i/N}$. We use N -LimTDD as a shorthand for \mathcal{XP}_N -LimTDD. Suppose \mathcal{F} and \mathcal{G} are two N -LimTDDs on the same index set and with the same index order. We write $\mathcal{F} \cong \mathcal{G}$ if $r_{\mathcal{F}} = r_{\mathcal{G}}$.

Theorem 1. *Suppose $\phi_{x_n \dots x_1}$ and $\gamma_{x_n \dots x_1}$ are two tensors with the same index set. Let \mathcal{F} and \mathcal{G} be the N -LimTDD representations of $\phi_{x_n \dots x_1}$ and $\gamma_{x_n \dots x_1}$ with the same index order. The following two conditions are equivalent:*

- 1) $\phi_{x_n \dots x_1}$ and $\gamma_{x_n \dots x_1}$ are \mathcal{XP}_N -isomorphic.
- 2) $r_{\mathcal{F}} = r_{\mathcal{G}}$ and $w_{\mathcal{F}} = O \cdot w_{\mathcal{G}} \cdot g$ for some $O \in \mathcal{XP}_N$ and some $g \in \text{Stab}(\Phi(r_{\mathcal{G}}))$.

Proof. $2 \Rightarrow 1$ follows directly from the definition. We prove $1 \Rightarrow 2$ by induction on the tensor rank.

For rank 0 tensors, the claim holds trivially. Now assume it holds for rank $n-1$, and consider the rank- n case. Given that $|\phi_{x_n \dots x_1}\rangle\rangle = O|\gamma_{x_n \dots x_1}\rangle\rangle$ with $O = X^{b_n} P^{z_n} \otimes w$, we show $r_{\mathcal{F}} = r_{\mathcal{G}}$, and $w_{\mathcal{F}} = O \cdot w_{\mathcal{G}} \cdot g$ for some $g \in \text{Stab}(\Phi(r_{\mathcal{G}}))$.

Suppose $\mathcal{G}_{x_n=0} = \xrightarrow{w_0} \textcircled{v_0}$ and $\mathcal{G}_{x_n=1} = \xrightarrow{w_1} \textcircled{v_1}$. Then $\mathcal{G} = \text{loc_norm}(x_n, \xrightarrow{w_0} \textcircled{v_0}, \xrightarrow{w_1} \textcircled{v_1}) = (w_{\mathcal{G}}, r_{\mathcal{G}})$, because \mathcal{G} is normalized.

According to the value of b_n , there are two cases to examine:

Case 1: If $b_n = 0$, then the components satisfy:

$$\Phi(\mathcal{F}_{x_n=0}) = \phi_{x_n=0} = w\gamma_{x_n=0} = w\Phi(\mathcal{G}_{x_n=0}),$$

$$\Phi(\mathcal{F}_{x_n=1}) = \phi_{x_n=1} = \omega^{2z_n} \cdot w\gamma_{x_n=1} = \omega^{2z_n} \cdot w\Phi(\mathcal{G}_{x_n=1}).$$

By the induction hypothesis, there exist $g_0 \in \text{Stab}(v_0)$ and $g_1 \in \text{Stab}(v_1)$ such that:

$$\mathcal{F}_{x_n=0} = \xrightarrow{w \cdot w_0 \cdot g_0} \textcircled{v_0} \text{ and } \mathcal{F}_{x_n=1} = \xrightarrow{\omega^{2z_n} w \cdot w_1 \cdot g_1} \textcircled{v_1}.$$

Because

$$\mathcal{F} = \text{loc_norm}(x_n, \xrightarrow{w \cdot w_0 \cdot g_0} \textcircled{v_0}, \xrightarrow{\omega^{2z_n} w \cdot w_1 \cdot g_1} \textcircled{v_1}),$$

applying Lemma 2 in the order (i), (ii), and (iv), we conclude $\mathcal{F} \cong \text{loc_norm}(x_n, \xrightarrow{w_0} \textcircled{v_0}, \xrightarrow{w_1} \textcircled{v_1}) = \mathcal{G}$.

Case 2: If $b_n = 1$, then the components satisfy:

$$\Phi(\mathcal{F}_{x_n=0}) = \phi_{x_n=0} = \omega^{2z_n} \cdot w\gamma_{x_n=1} = \omega^{2z_n} \cdot w\Phi(\mathcal{G}_{x_n=1}),$$

$$\Phi(\mathcal{F}_{x_n=1}) = \phi_{x_n=1} = w\gamma_{x_n=0} = w\Phi(\mathcal{G}_{x_n=0}).$$

There exist $g_0 \in \text{Stab}(v_0)$ and $g_1 \in \text{Stab}(v_1)$ such that:

$$\mathcal{F}_{x_n=0} = \xrightarrow{\omega^{2z_n} w \cdot w_1 \cdot g_1} \textcircled{v_1} \text{ and } \mathcal{F}_{x_n=1} = \xrightarrow{w \cdot w_0 \cdot g_0} \textcircled{v_0}.$$

Because

$$\mathcal{F} = \text{loc_norm}(x_n, \xrightarrow{\omega^{2z_n} w \cdot w_1 \cdot g_1} \textcircled{v_1}, \xrightarrow{w \cdot w_0 \cdot g_0} \textcircled{v_0}),$$

applying Lemma 2 in the order (i), (ii), (iii), and (iv), we conclude

$$\mathcal{F} \cong \text{loc_norm}(x_n, \xrightarrow{w_0} \textcircled{v_0}, \xrightarrow{w_1} \textcircled{v_1}) = \mathcal{G}.$$

This means that, for both cases, $r_{\mathcal{F}} = r_{\mathcal{G}}$. Since $w_{\mathcal{F}} \cdot \Phi(r_{\mathcal{F}}) = |\phi_{x_n \dots x_1}\rangle\rangle = O \cdot |\gamma_{x_n \dots x_1}\rangle\rangle = O \cdot w_{\mathcal{G}} \cdot \Phi(r_{\mathcal{G}})$, we have $w_{\mathcal{G}}^\dagger \cdot O^\dagger \cdot w_{\mathcal{F}} \cdot \Phi(r_{\mathcal{G}}) = \Phi(r_{\mathcal{G}})$. Let $g = w_{\mathcal{G}}^\dagger \cdot O^\dagger \cdot w_{\mathcal{F}}$. Then $g \in \text{Stab}(\Phi(r_{\mathcal{G}}))$ and $w_{\mathcal{F}} = O \cdot w_{\mathcal{G}} \cdot g$. \square

This theorem shows that two \mathcal{XP}_N -isomorphic tensors have isomorphic N -LimTDD representations.

Since the number of operators is growing as N increases, any N -LimTDD is also an $(N+1)$ -LimTDD. We have the following natural corollary:

Corollary 1. *For any tensor ϕ and any $N \geq 0$, let \mathcal{F} be its $(N+1)$ -LimTDD representation and \mathcal{G} its N -LimTDD representation. Then, $\text{size}(\mathcal{F}) \leq \text{size}(\mathcal{G})$, where $\text{size}(\mathcal{F})$ and $\text{size}(\mathcal{G})$ denote the number of nodes in \mathcal{F} and \mathcal{G} , respectively.*

Regarding quantum states, LIMDDs are equivalent to 2-LimTDDs. For general tensors, 1-LimTDDs offer a more compact representation than TDDs, as they enable further compression of tensors that differ only by a series of X operators. We could denote TDD as 0-LimTDD with a little abuse of the notation. This leads to the following result.

Theorem 2 (LimTDD vs. TDD & LIMDD). 1) *Let \mathcal{F} be the LimTDD representation and \mathcal{G} the TDD representation of the same tensor $\phi_{x_n \dots x_1}$ with the same index order. Then, $\text{size}(\mathcal{F}) \leq \text{size}(\mathcal{G})$.*

2) *Let \mathcal{F} be the LimTDD representation and \mathcal{G} the LIMDD representation of the same quantum state $|\phi_{x_n \dots x_1}\rangle$ with the same index (qubit) order. Then, $\text{size}(\mathcal{F}) \leq \text{size}(\mathcal{G})$.*

A. Tower LimTDD

A LimTDD is in *tower form* (illustrated in Fig. 4) if for every internal v , the 0- and 1-successors are identical, i.e., $\text{low}(v) = \text{high}(v)$. In such cases, the tensors represented by the low and high edges of any internal node v differ only by a local operator. Conversely, if two tensors differ only by a local operator, they could be represented as two LimTDDs sharing the same root node. This leads to the following corollary:

Corollary 2 (Tower LimTDD). *A tensor $\phi_{x_n \dots x_1}$ can be represented as a tower LimTDD if and only if for every $i \in \{n, \dots, 1\}$, there exists an operator $O_i \in \mathcal{O}(i-1)$ such that: $|\phi_{x_n \dots x_i=0 \dots 00}\rangle\rangle = O_i |\phi_{x_n \dots x_i=0 \dots 01}\rangle\rangle$.*

In [18], it was shown that all stabilizer states admit tower-form representations using LIMDDs. Below, we identify more classes of quantum states that can be represented as tower-form LimTDDs and highlight cases where LimTDDs exhibit exponentially better compactness over LIMDDs:

- 1) States prepared from $|0\rangle$ using the gate set $\{H, P_{N'}\}$ admit tower N -LimTDD representations for $N \geq 0$ and $N' > 0$.
- 2) States prepared from $|0\rangle$ using the gate set $\{X, CX, P_{N'}, CP_{N'}\}$ admit tower N -LimTDD representations for $N \geq 0$ and $N' > 0$.

- 3) States prepared from $|0\rangle$ using the gate set $\{H, CX, S\}$ admit tower N -LimTDD representations for $N \geq 2$.
- 4) States prepared from $|0\rangle$ using the gate set $\{H, P_{N'}, CP_{N'}\}$ with at most one H gate per qubit, admit tower N -LimTDD representations for $N \geq N' > 0$.

The first type of circuit generates no entanglement, while the second type produces no superposition. The third type constitutes Clifford circuits. For the fourth type, applying a single H gate per qubit preserves the tower form for computational basis states, and phase gates ($P_{N'}$) or controlled phase gates ($CP_{N'}$) retain this structure without disruption.

Remark 1. (1) Since LIMDD is equivalent to 2-LimTDD for quantum state representation and TDD corresponds to 0-LimTDD, the first two circuit types admit tower-form representations across all three decision diagrams. The third type (Clifford circuits) requires $N \geq 2$ for tower-form representation in LimTDD. Notably, the fourth type demonstrates an exponential advantage of LimTDD over LIMDD and TDD, as evidenced experimentally.

(2) The theoretical compactness assumes strong canonicity, necessitating full stabilizer checks in Algorithm 1 (lines 5 and 6). In practice, our implementation omits these checks, which may result in marginally larger node counts than theoretically predicted. However, experimental data indicate this rarely exceeds TDD/LIMDD sizes.

VI. APPLICATIONS

LimTDD aims to provide a more compact and efficient representation for tensors and quantum states, which can significantly enhance the efficiency of various tasks in quantum computing and tensor network computations. In this section, we explore several key applications where LimTDD's compactness translates into practical advantages.

A. Quantum Circuit Simulation

Quantum circuit simulation is a fundamental task in quantum computing, essential for understanding the behavior of quantum circuits, debugging, and optimizing circuit designs. However, simulating quantum circuits on classical computers is challenging due to the exponential growth of the state space with the number of qubits.

LimTDD's compact representation allows it to handle larger quantum circuits with fewer resources. By exploiting tensor isomorphisms and using the XP-stabilizer group, LimTDD can represent quantum states and operations more efficiently, reducing the memory and computational requirements for simulation.

B. Equivalence Checking of Quantum Circuits

Equivalence checking is a critical task in quantum circuit design and verification, where two circuits are deemed equivalent if they produce the same output state for any given input state. LimTDD's compact representation significantly enhances the efficiency of this task.

By leveraging the XP-stabilizer group and local invertible maps, LimTDD can merge structurally similar tensors, reducing

the complexity of the decision diagram. This allows for checking the equivalence of two circuits with less memory space, and enables checking larger circuits.

C. Model Checking of Quantum Circuits

Model checking is another important application in quantum circuit verification, where the correctness of a quantum circuit is verified against a formal specification. LimTDD's compact representation allows for more efficient model checking by reducing the computational complexity of the verification process.

D. Further Applications

Beyond the specific applications mentioned above, LimTDD's compact representation can be applied to a wide range of tasks in quantum computing and tensor network computations. For instance, LimTDD can be used for:

- 1) Quantum State Preparation: Efficiently representing and manipulating quantum states is crucial for tasks such as state preparation. LimTDD's compactness allows for more efficient handling of these tasks.
- 2) Quantum Algorithm Design: LimTDD can aid in the design and optimization of quantum algorithms by providing a more efficient way to represent and manipulate quantum operations.
- 3) Tensor Network Computations: LimTDD's integration of tensor representations and local invertible maps makes it a powerful tool for general tensor network computations, which are widely used in fields such as quantum many-body physics and machine learning.

In the next section, we will compare the efficiency of LimTDD and TDD through experiments, focusing on quantum circuit simulation and functionality construction.

VII. EXPERIMENTS

We conducted a comprehensive evaluation of LimTDD, TDD, and LIMDD, measuring their efficiency in quantum circuit simulation and functionality construction. Our benchmark suite includes:

- Standard quantum algorithms: QFT, GHZ, and Grover circuits
- Random Clifford circuits
- Random Clifford+T circuits with varying T-gate densities

For each method, we recorded:

- Total execution time
- Maximum node count during computation
- Memory usage

All three tools were implemented in C++ and executed on the same platform (Intel(R) Core(TM) i5-13600KF CPU, 32GB RAM, GCC compiler). The LIMDD implementation is from MQT-bench [14] (<https://github.com/cda-tum/mqt-limdd>) and the TDD implementation is from (https://github.com/Veriqc/TDD_C). All three tools use the same index (qubit) order, and all tensors (quantum gates) were processed from left to right according to the circuit, without any additional optimizations. Note that, because LIMDD can not be used to construct the functionality of a quantum circuit, we only compare TDD and LimTDD for this task.

A. Simulation with Random Clifford + T Circuits

We first compare the three decision diagrams using random Clifford + T circuits, a universal gate set commonly used in quantum computation. The probability of T-gate occurrence is set to 0.02, and the circuits are simulated with the input state $|0 \cdots 0\rangle$. These circuits, 1000 in total, are randomly generated from the gate set $\{X, Y, Z, S, H, CX, T\}$, each consisting of 10 qubits and 400 gates. The corresponding experiment data is shown in Fig. 8. The experiments indicate that LimTDD is more compact than LIMDD for these circuits, and TDD performs the worst, with LimTDD requiring fewer nodes and less computation time.

We also conducted experiments on 1000 randomly generated circuits with 20 qubits and 600 gates, where the trend is even more pronounced. In these experiments, the average runtime for LimTDD was less than 0.25 seconds, over 10 times shorter than TDD and 100 times shorter than LIMDD. Furthermore, LimTDD consistently required fewer nodes, with an average maximum of approximately 800 nodes, significantly less than the approximately 10^4 and 10^5 nodes for TDD and LIMDD, respectively. Notably, LimTDD outperformed the other methods in terms of efficiency and compactness in 992 out of 1000 experiments. These results highlight LimTDD’s superior performance for Clifford + T circuits, demonstrating its practical advantages in quantum computation. However, we also observed that LIMDD performed worse than TDD in this group of experiments, possibly indicating implementation issues with the current version of LIMDD, or that it is not fully implemented according to the methodologies in [18].

B. Functionality Construction

We then compare the three decision diagrams—TDD, LimTDD, and LIMDD—in their ability to construct quantum circuit functionality. For this comparison, we employ several common quantum algorithms, including Quantum Fourier Transform (QFT), GHZ state preparation, and Grover’s algorithm. Functionality representation, which provides a precise description of quantum circuit behaviour, is essential for tasks such as equivalence checking. All circuits are taken from the MQT benchmark suite. Since LIMDD cannot directly represent quantum circuit functionality, we only present results for TDD and LimTDD.

The overall comparison results are summarized in Table II. In the worst cases, LimTDD matches TDD’s node count and takes slightly longer to compute, as its internal operations are more complex. However, LimTDD significantly outperforms TDD in node count for most scenarios. For example, for the ‘qpeexact_10’ circuit, LimTDD requires only 68,010 nodes, while TDD needs 466,988 nodes—approximately seven times more. Similar trends are observed for circuits like ‘ae’ and ‘dj’. In the best cases, such as the ‘qft’ circuit, LimTDD shows exponential improvement in compactness and efficiency compared to TDD. For the ‘qft_10’ circuit, LimTDD needs only 21 nodes, while TDD requires 525,311 nodes. When an increase to 12 qubits, LimTDD still completes the task with just 25 nodes, while TDD needs 8392703 nodes.

TABLE II
THE EXPERIMENT DATA FOR FUNCTIONALITY OF SOME COMMON ALGORITHMS.

Benchmarks	TDD		LimTDD	
	Time (s)	Nodes	Time (s)	Nodes
ae_10	1.819	174802	4.651	131111
dj_60	0.079	356	0.061	121
dj_120	0.291	716	0.285	241
ghz_60	0.012	355	0.004	121
ghz_120	0.033	715	0.007	241
graphstate_30	0.129	34301	0.004	61
graphstate_60	75.455	3798765	0.011	121
grover-noancilla_7	23.187	16384	81.636	16384
portfoliovqe_8	3.425	65536	5.174	65536
qft_10	2.416	525311	0.019	21
qft_12	137.745	8392703	0.074	25
qftentangled_10	5.840	567597	5.762	153158
qnn_8	1.938	65536	8.483	65536
qpeexact_10	0.575	26978	0.138	3928
qpeexact_12	14.793	466988	2.261	68010
qpeinexact_10	1.309	87334	0.345	15424
qpeinexact_12	60.244	1379333	11.398	237193
qwalk-noancilla_7	3.013	15379	5.606	11282

C. The Influence of Operator Precision N

In this subsection, we investigate the impact of precision N on the compactness of LimTDDs when simulating quantum circuits. We consider four types of circuits: Clifford, Clifford+T ($diag(1, e^{2\pi i/8})$), Clifford+ \sqrt{T} ($diag(1, e^{2\pi i/16})$), and Clifford+ $\sqrt[4]{T}$ ($diag(1, e^{2\pi i/32})$). These circuits are chosen because their minimum rotation angles decrease progressively, potentially necessitating higher precision for accurate simulation. Each circuit comprises 400 gates and 15 qubits, with rotation gate proportions set at 0.1 and 0.3. We simulate 200 random circuits for each setting and record the average maximum number of nodes required. The results are summarized in Fig. 10.

As illustrated in the figure, the average number of nodes decreases with increasing precision N for all circuit types. However, this trend ceases when $N > 4$ for Clifford+T circuits and $N > 8$ for Clifford+ \sqrt{T} circuits. For Clifford+ $\sqrt[4]{T}$ circuits, the trend persists up to $N = 32$. On one hand, this demonstrates that increasing N enhances the compactness of LimTDDs, highlighting the necessity of introducing LimTDDs for efficient simulation. However, it also reveals the limitations of this approach: after N reaches a certain threshold, further increases do not improve the compactness of the decision diagram. This is because the minimum argument of the matrix elements corresponding to the circuit imposes a fundamental limit, necessitating alternative techniques to address this limitation.

D. An Example of LimTDD’s Exponential Advantage

The impact of precision N on LimTDD compactness for different types of circuits, combined with the theoretical comparisons in Section V, has motivated us to identify circuits that exhibit an exponential advantage over other decision

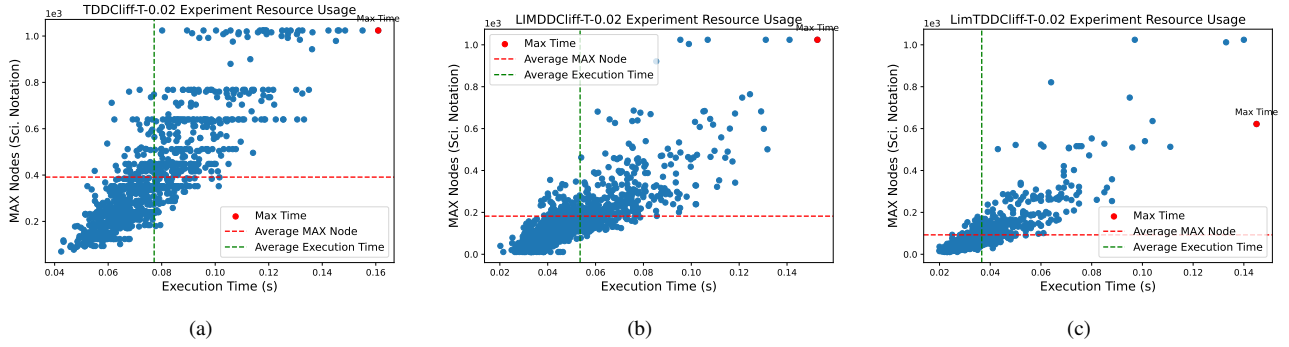


Fig. 8. Comparison of time and space efficiency for TDD, LIMDD, and LimTDD over 1000 random Clifford+T circuits (10 qubits, 400 gates). The y -axes for node counts are scaled using scientific notation (units: 10^3).

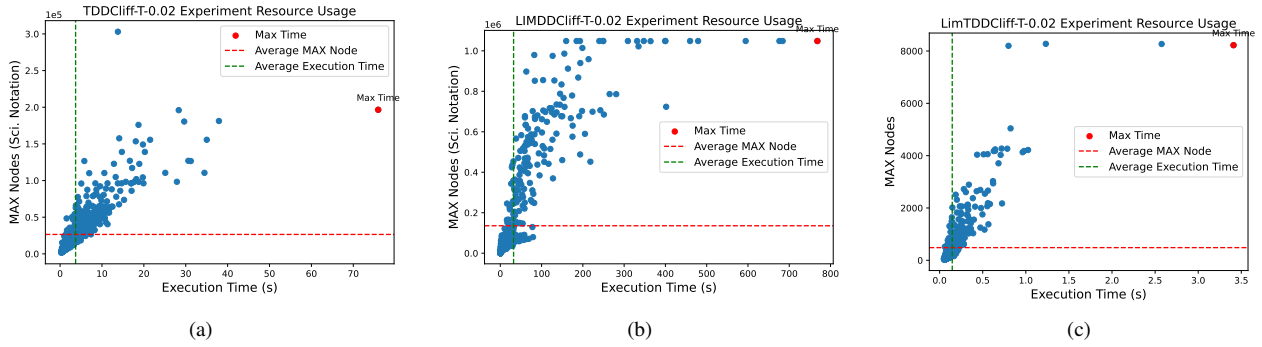


Fig. 9. Comparison of time and space efficiency for TDD, LimTDD, and LIMTDD over 1000 random Clifford+T circuits (20 qubits, 600 gates). The y -axes for TDD and LimTDD node counts are scaled using scientific notation (units: 10^5 for TDD, 10^6 for LIMDD).

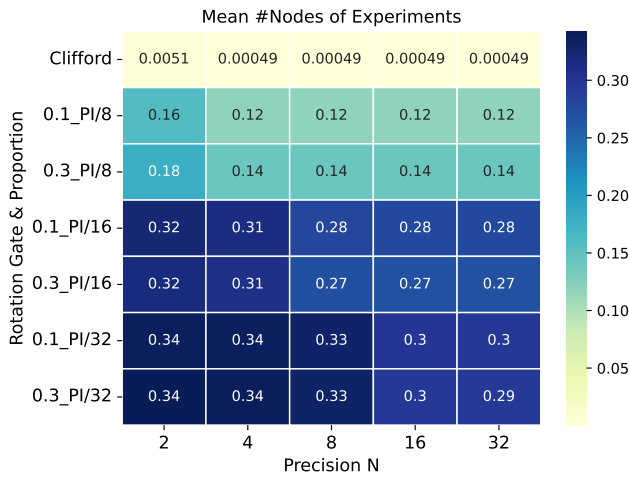


Fig. 10. Results of simulating random circuits using LimTDD with different precision levels (N th root of unity). Rows represent different circuit types (Clifford, and Clifford with various rotation gates and proportions; for example, 0.1_PI/8 represents a gate $\text{diag}(1, e^{2\pi i/8})$ with proportions 0.1). Data shows the compression ratio, defined as the number of nodes divided by $2^{\#\text{qubit}}$.

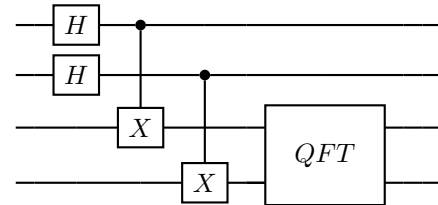


Fig. 11. A quantum circuit for preparing $(I \otimes QFT) |\Psi\rangle$, where $|\Psi\rangle = \frac{1}{\sqrt{2^n}} \sum_{i=0}^{2^n-1} |ii\rangle$.

$\{2^0, 2^1, \dots, 2^{n-3}\}$. Fig. 12 presents the experimental results for simulating the circuit depicted in Fig. 11. The circuit applies an $I \otimes QFT$ operation on the maximally entangled state $|\Psi\rangle = \frac{1}{\sqrt{2^n}} \sum_{i=0}^{2^n-1} |ii\rangle$. The results show that LimTDD is exponentially more efficient and compact than TDD and LIMDD. For $n = 15$ qubits, LimTDD completes the simulation in just 0.5 seconds, with a maximum node count of 31. In contrast, TDD takes 8.6 seconds, and LIMDD requires 37 seconds. The node counts for TDD and LIMDD are 98,302 and 32,797, respectively. This highlights LimTDD's significant advantages in computational efficiency and memory usage.

VIII. CONCLUSION

This paper presented LimTDD, a novel decision diagram that integrates tensor representations with local invertible maps (LIMs) to achieve more compact and efficient representations of

diagrams, such as TDD and LIMDD. This subsection provides such an example, which incorporates the Quantum Fourier Transform (QFT) as its core component. Note that a QFT circuit includes gates of the form Controlled- $\sqrt[k]{T}$, for k in

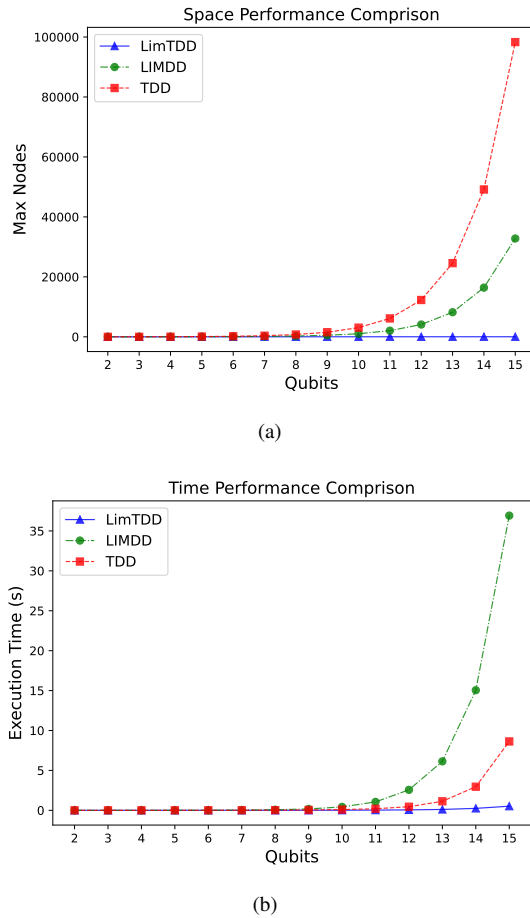


Fig. 12. Time and space comparison of TDD, LimDD, and LimTDD in simulating the circuit shown in Fig. 11. LimTDD used a precision (N) of $2^{15} = 32,768$.

quantum states and general tensors. By generalizing LIMDD’s use of Pauli operators to the more flexible XP-stabilizer group, LimTDD extends applicability beyond quantum states to arbitrary tensor networks while maintaining superior compression. Theoretical analysis demonstrated that LimTDD is strictly more compact than TDD and LIMDD, with exponential advantages in the best-case scenarios—such as circuits involving QFT and controlled-phase gates. Experimental results confirmed these improvements, showing significant reductions in node counts and computation time for quantum circuit simulation and functionality computation tasks.

Future work will focus on extending LimTDD’s operator support to include multi-qubit gates and arbitrary diagonal operations, further enhancing its compression capabilities. Additionally, we plan to investigate applications in broader tensor network computations beyond quantum computing. These advancements will solidify LimTDD as a versatile and powerful tool for efficient representation and manipulation of high-dimensional data in quantum and classical settings.

REFERENCES

[1] BAHAR, R. I., FROHM, E. A., GAONA, C. M., HACHTEL, G. D., MACII, E., PARDO, A., AND SOMENZI, F. Algebraic decision diagrams and their applications. *Formal methods in system design* 10 (1997), 171–206.

[2] BIAMONTE, J. Lectures on quantum tensor networks. *arXiv preprint arXiv:1912.10049* (2019).

[3] BURGHOLZER, L., AND WILLE, R. Advanced equivalence checking for quantum circuits. *IEEE Transactions on Computer-Aided Design of Integrated Circuits and Systems* 40, 9 (2020), 1810–1824.

[4] BURGHOLZER, L., AND WILLE, R. QCEC: A JKQ tool for quantum circuit equivalence checking. *Software Impacts* 7 (2021), 100051.

[5] CAO, Y., ROMERO, J., OLSON, J. P., DEGROOTE, M., JOHNSON, P. D., KIEFEROVÁ, M., KIVLICHAN, I. D., MENKE, T., PEROPADRE, B., SAWAYA, N. P., ET AL. Quantum chemistry in the age of quantum computing. *Chemical reviews* 119, 19 (2019), 10856–10915.

[6] HONG, X., FENG, Y., LI, S., AND YING, M. Equivalence checking of dynamic quantum circuits. In *2022 IEEE/ACM International Conference On Computer Aided Design (ICCAD)* (2022), pp. 1–8.

[7] HONG, X., YING, M., FENG, Y., ZHOU, X., AND LI, S. Approximate equivalence checking of noisy quantum circuits. In *2021 58th ACM/IEEE Design Automation Conference (DAC)* (2021), IEEE, pp. 637–642.

[8] HONG, X., ZHOU, X., LI, S., FENG, Y., AND YING, M. A tensor network based decision diagram for representation of quantum circuits. *ACM Transactions on Design Automation of Electronic Systems (TODAES)* 27, 6 (2022), 1–30.

[9] MARKOV, I. L., AND SHI, Y. Simulating quantum computation by contracting tensor networks. *SIAM Journal on Computing* 38, 3 (2008), 963–981.

[10] MATO, K., HILLMICH, S., AND WILLE, R. Mixed-dimensional qudit state preparation using edge-weighted decision diagrams. In *Proceedings of the 61st ACM/IEEE Design Automation Conference, DAC 2024, San Francisco, CA, USA, June 23-27, 2024* (2024), V. De, Ed., ACM, pp. 50:1–50:6.

[11] NIELSEN, M. A., AND CHUANG, I. L. *Quantum computation and quantum information*. Cambridge University Press, 2010.

[12] NIEMANN, P., WILLE, R., MILLER, D. M., THORNTON, M. A., AND DRECHSLER, R. QMDDs: Efficient quantum function representation and manipulation. *IEEE Transactions on Computer-Aided Design of Integrated Circuits and Systems* 35, 1 (2015), 86–99.

[13] PRESKILL, J. Quantum computing in the NISQ era and beyond. *Quantum* 2 (2018), 79.

[14] QUETSCHLICH, N., BURGHOLZER, L., AND WILLE, R. MQT Bench: Benchmarking software and design automation tools for quantum computing. *Quantum* (2023). MQT Bench is available at <https://www.cda.cit.tum.de/mqtbench/>.

[15] REBENTROST, P., MOHSENI, M., AND LLOYD, S. Quantum support vector machine for big data classification. *Physical review letters* 113, 13 (2014), 130503.

[16] VIAMONTES, G. F., MARKOV, I. L., AND HAYES, J. P. Improving gate-level simulation of quantum circuits. *Quantum Information Processing* 2, 5 (2003), 347–380.

[17] VIAMONTES, G. F., MARKOV, I. L., AND HAYES, J. P. High-performance QuIDD-based simulation of quantum circuits. In *Proceedings Design, Automation and Test in Europe Conference and Exhibition* (2004), vol. 2, IEEE, pp. 1354–1355.

[18] VINKHUIJZEN, L., COOPMANS, T., ELKOUSS, D., DUNJKO, V., AND LAARMAN, A. LIMDD: A decision diagram for simulation of quantum computing including stabilizer states. *Quantum* 7 (2023), 1108.

[19] VINKHUIJZEN, L., GRURL, T., HILLMICH, S., BRAND, S., WILLE, R., AND LAARMAN, A. Efficient implementation of LIMDDs for quantum circuit simulation. In *International Symposium on Model Checking Software* (2023), Springer, pp. 3–21.

[20] WANG, S.-A., LU, C.-Y., TSAI, I.-M., AND KUO, S.-Y. An XQDD-based verification method for quantum circuits. *IEICE transactions on fundamentals of electronics, communications and computer sciences* 91, 2 (2008), 584–594.

[21] WEBSTER, M. A., BROWN, B. J., AND BARTLETT, S. D. The XP Stabiliser Formalism: a Generalisation of the Pauli Stabiliser Formalism with Arbitrary Phases. *Quantum* 6 (Sept. 2022), 815.

[22] WILLE, R., BERENT, L., FORSTER, T., KUNASAIKARAN, J., MATO, K., PEHAM, T., QUETSCHLICH, N., ROVARA, D., SANDER, A., SCHMID, L., SCHÖNBERGER, D., STADE, Y., AND BURGHOLZER, L. The MQT handbook : A summary of design automation tools and software for quantum computing. In *IEEE International Conference on Quantum Software, QSW 2024, Shenzhen, China, July 7-13, 2024* (2024), R. N. Chang, C. K. Chang, J. Yang, Z. Jin, M. Sheng, J. Fan, K. Fletcher, Q. He, I. Faro, F. Leymann, J. Barzen, S. de la Puente, S. Feld, M. Wimmer, N. Atukorala, H. Wu, D. Elkouss, J. García-Alonso, and A. Sarkar, Eds., IEEE, pp. 1–8.

[23] ZHANG, Q., SALIGANE, M., KIM, H.-S., BLAAUW, D., TZIMPRAGOS, G., AND SYLVESTER, D. Quantum circuit simulation with fast tensor

decision diagram. In *2024 25th International Symposium on Quality Electronic Design (ISQED)* (2024), pp. 1–8.

APPENDIX

A. Operations of XP-Operators

Understanding the group generated by XP-operators requires characterizing the unit operator, multiplication, and inverses of XP-operators. We will need the following notation: for any integer vector $\mathbf{z} \in \mathbb{Z}^n$, we write $D_N(\mathbf{z}) := XP_N(\sum_i \mathbf{z}[i]|\mathbf{0}|-\mathbf{z})$, denoting the antisymmetric operator for \mathbf{z} .

First, we note that

$$I = XP_N(0|\mathbf{0}|\mathbf{0}), \quad -I = XP_N(N|\mathbf{0}|\mathbf{0}).$$

Second, suppose $\mathbf{u}_1 = (p_1|\mathbf{x}_1|\mathbf{z}_1)$ and $\mathbf{u}_2 = (p_2|\mathbf{x}_2|\mathbf{z}_2)$. The multiplication of two XP-operators $XP_N(\mathbf{u}_1)$ and $XP_N(\mathbf{u}_2)$ can then be computed as:

$$XP_N(\mathbf{u}_1)XP_N(\mathbf{u}_2) = XP_N(\mathbf{u}_1 + \mathbf{u}_2)D_N(2\mathbf{x}_2\mathbf{z}_1), \quad (11)$$

where addition and multiplication of vectors are performed component-wise and with proper modulus. That is:

$$\begin{aligned} (\mathbf{a} + \mathbf{b})[j] &= \mathbf{a}[j] + \mathbf{b}[j] \pmod{\mathbf{m}[j]}, \\ (\mathbf{a}\mathbf{b})[j] &= \mathbf{a}[j]\mathbf{b}[j] \pmod{\mathbf{m}[j]}, \end{aligned}$$

where \mathbf{m} is a $(2n + 1)$ -dimensional vector such that

$$\mathbf{m}[j] = \begin{cases} 2N, & \text{if } j = 0 \\ 2, & \text{if } 1 \leq j \leq n \\ N, & \text{if } n + 1 \leq j \leq 2n \end{cases}$$

Lastly, the inverse of the operator $XP_N(p|\mathbf{x}|\mathbf{z})$ is given by:

$$XP_N(-p|\mathbf{x}|-\mathbf{z})D_N(-2\mathbf{x}\mathbf{z}). \quad (12)$$

Furthermore, since the X -components of $D_N(2\mathbf{x}_2\mathbf{z}_1)$ and $D_N(-2\mathbf{x}\mathbf{z})$ are $\mathbf{0}$, right multiplication of these operators in (11) and (12) only modifies the phase and Z -components of the original XP-operator.

B. Calculate $Stab(v)$

In this subsection, we show how to calculate a generating set for $Stab(v)$ for an internal node v and calculate $\min_{g_0 \in Stab(r_{\mathcal{F}_0}), g_1 \in Stab(r_{\mathcal{F}_1})} g_0^\dagger \cdot w \cdot g_1$.

Suppose v is a node with two successors v_0, v_1 , and the label on the high edge is h ; then there are two cases. First, if $v_0 \neq v_1$, then only operators of the form $P^z \otimes g$ can be in $Stab(v)$, and g must stabilise v_0 and $\omega^{2z}h^\dagger gh$ must stabilise v_1 for some z . Otherwise, operators of the form $P^z \otimes g$ and $XP^z \otimes g$ all can be in $Stab(v)$. More specifically:

(1) If $v_0 \neq v_1$, $Stab(v) = \{P^z \otimes g | g \in Stab(v_0) \text{ and } \omega^{2z}h^\dagger gh \in Stab(v_1)\}$;

(2) If $v_0 = v_1$, $Stab(v) = \{P^z \otimes g | g \in Stab(v_0) \text{ and } \omega^{2z}h^\dagger gh \in Stab(v_1)\} \cup \{XP^z \otimes g | hg \in Stab(v_0) \text{ and } \omega^{2z}gh \in Stab(v_1)\}$.

For the rank 1 cases, the tensor represented by a normalized node v can only be $[1, r]^\top$, where $r \in \mathbb{R}$, and $0 \leq r \leq 1$. Then, there are three cases:

- (1) If $r = 0$, then $Stab(v) = \langle P \rangle$;
- (2) If $r = 1$, then $Stab(v) = \langle X \rangle$;

(3) $Stab(v) = \emptyset$, otherwise.

Then, G_0 and G_1 are the generating sets of $Stab(v_0)$ and $Stab(v_1)$ ignoring their phase components, to calculate a generating set for $Stab(v)$, we only need to calculate $\langle G_0 \rangle \cap \langle hG_1h^\dagger \rangle$ and then adding a suitable phase for each item. Note that the intersection of two groups of XP Stabilizers can be calculated by solving a system of linear equations $S_{X_0}^{a_0} S_{Z_0}^{b_0} = S_{X_1}^{a_1} S_{Z_1}^{b_1}$ in the canonical generating set form, and the time complexity is polynomial with n . The minimum value of $g_0^\dagger \cdot w \cdot g_1$ for $g_0 \in Stab(r_{\mathcal{F}_0}), g_1 \in Stab(r_{\mathcal{F}_1})$ can also be calculated using their canonical generating set form.

Note that in lines 9 and 10 of Algorithm 1, we are supposed to find the minimal element of the set

$$\{g_0^\dagger \cdot w_{\mathcal{F}_0}^\dagger \cdot w_{\mathcal{F}_1} \cdot g_1 \mid g_0 \in Stab(r_{\mathcal{F}_0}), g_1 \in Stab(r_{\mathcal{F}_1})\}$$

and

$$\{g_1^\dagger \cdot w_{\mathcal{F}_1}^\dagger \cdot w_{\mathcal{F}_0} \cdot g_0 \mid g_0 \in Stab(r_{\mathcal{F}_0}), g_1 \in Stab(r_{\mathcal{F}_1})\},$$

which is useful for making the representation canonical. Although it can be done with a time complexity polynomial with n , we still think it is a little complicated. In our implementation, we will not obey this routine, and we will suppose $Stab(r_{\mathcal{F}_0}) = Stab(r_{\mathcal{F}_1}) = \{I\}$, then (iii) in Lemma 2 will be changed to

$$\text{loc_norm}\left(x, \xrightarrow{w_1} \textcircled{v_1}, \xrightarrow{w_0} \textcircled{v_0}\right) = ((X \otimes I) \cdot w, \text{node}),$$

if $w_0^\dagger w_1 \neq w_1^\dagger w_0$ or $v_0 \neq v_1$; and (iv) needs $w_0 \cdot g_0$ and $w_1 \cdot g_1$ to remain in the same order as w_0 and w_1 . This damages the property of canonical to some extent, but it is not serious according to our experimental data. In fact, the complete canonicity is not a very necessary matter for simulation or for verification of quantum circuits since two quantum circuits are equivalent if and only if $\text{tr}(UV^\dagger) = 2^n$ and equivalent up to global phase if and only if $|\text{tr}(UV^\dagger)| = 2^n$. Here, U and V represent the matrix representation of the two circuits, n is the number of qubits, $\text{tr}(UV^\dagger)$ is a scalar and can be calculated by reversing one of the circuits and connect the input and output of the two circuits.